

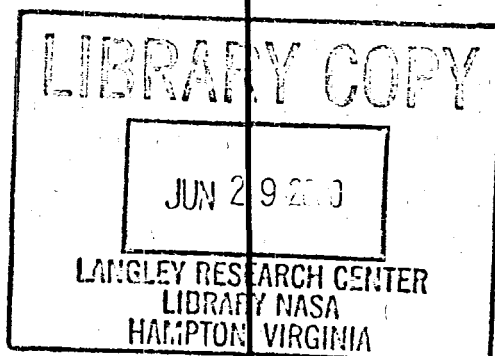
January 1992

NASA-TP-3129

NASA-TP-3129 19940028359

# A Finite-Difference Approximate-Factorization Algorithm for Solution of the Unsteady Transonic Small-Disturbance Equation

John T. Batina



~~RESTRICTED~~

~~FOR EARLY DOMESTIC DISSEMINATION~~

Because of its significant early commercial potential, this information, which has been developed under a U.S. Government program, is being disseminated within the United States in advance of general publication. This information may be duplicated and used by the recipient with the express limitation that it not be published. Release of this information to other domestic entities by the recipient shall be made subject to these limitations.

Foreign release may be made only with prior NASA approval and appropriate export licenses. This legend shall be marked on any reproduction of this information in whole or in part.

Review for general release January 31, 1994



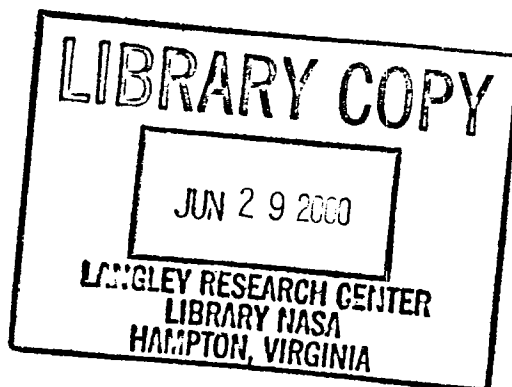
**NASA  
Technical  
Paper  
3129**

1992



**A Finite-Difference  
Approximate-Factorization  
Algorithm for Solution  
of the Unsteady Transonic  
Small-Disturbance Equation**

John T. Batina  
*Langley Research Center  
Hampton, Virginia*



National Aeronautics and  
Space Administration  
Office of Management  
Scientific and Technical  
Information Program



# Contents

Abstract . . . . .	1
Introduction . . . . .	1
Symbols . . . . .	1
Governing Equations . . . . .	3
TSD Equation . . . . .	3
Coordinate Transformation . . . . .	4
Boundary Conditions . . . . .	4
Entropy Model . . . . .	6
Alternative streamwise flux . . . . .	6
Pressure correction . . . . .	6
Modified wake boundary condition . . . . .	7
Vorticity Model . . . . .	7
Modified velocity vector . . . . .	7
Pressure correction . . . . .	8
Modified wake boundary condition . . . . .	8
Approximate-Factorization Algorithm . . . . .	8
General Description . . . . .	8
Mathematical Formulation . . . . .	9
Time-Linearization Step . . . . .	9
Difference Equations for the Disturbance Velocity . . . . .	9
At Half-Node Points $(i \pm 1/2, j, k)$ . . . . .	10
At Half-Node Points $(i, j \pm 1/2, k)$ . . . . .	11
At Half-Node Points $(i, j, k \pm 1/2)$ . . . . .	12
Difference Equations for the Grid Metrics . . . . .	13
At Grid Points $(i, j, k)$ . . . . .	13
At Half-Node Points $(i \pm 1/2, j, k)$ . . . . .	13
At Half-Node Points $(i, j \pm 1/2, k)$ . . . . .	14
Difference Equations for the Left-Hand-Side Operators . . . . .	14
$L_\xi$ Operator . . . . .	14
$L_\eta$ Operator . . . . .	17
$L_\zeta$ Operator . . . . .	19
Difference Equations for the Residual . . . . .	23
$\partial g_0 / \partial t$ Term . . . . .	24
$\partial g_1 / \partial \xi$ Term . . . . .	24
$\partial g_2 / \partial \eta$ Term . . . . .	26
$\partial g_3 / \partial \zeta$ Term . . . . .	26
Difference Equations for the Far-Field Boundary Conditions . . . . .	27
Upstream Boundary . . . . .	27

Downstream Boundary . . . . .	27
Far-Spanwise Boundary . . . . .	28
Upper Boundary . . . . .	31
Lower Boundary . . . . .	32
Concluding Remarks . . . . .	33
References . . . . .	33

## Abstract

A time-accurate approximate-factorization (AF) algorithm is described for solution of the three-dimensional unsteady transonic small-disturbance equation. The AF algorithm consists of a time-linearization procedure coupled with a subiteration technique. The algorithm is the basis for the CAP-TSD (Computational Aeroelasticity Program-Transonic Small Disturbance) computer code, which was developed for the analysis of unsteady aerodynamics and aeroelasticity of realistic aircraft configurations. The paper describes details on the governing flow equations and boundary conditions, with an emphasis on documenting the finite-difference formulas of the AF algorithm.

## Introduction

Considerable research is being conducted presently to develop computational fluid dynamics methods for predicting unsteady transonic aerodynamics for aeroelastic applications (ref. 1.) The resulting computer codes are being developed to provide accurate methods of calculating unsteady air loads for the prediction of aeroelastic phenomena such as flutter and divergence. One of the most fully developed codes for analysis of transonic aeroelasticity, for example, is the CAP-TSD (Computational Aeroelasticity Program-Transonic Small Disturbance) computer code (ref. 2.) The code permits the calculation of unsteady flows about realistic aircraft configurations for analysis of aeroelasticity in the flutter-critical transonic speed range. It can treat configurations with general combinations of lifting surfaces and bodies.

The code uses a time-accurate approximate-factorization (AF) algorithm (refs. 3 and 4) developed for solution of the three-dimensional unsteady transonic small-disturbance (TSD) equation. The AF algorithm involves a time-linearization procedure coupled with a subiteration technique and is similar to the unsteady full-potential algorithm reported by Shankar et al. (ref. 5.) References 3 and 4 show the AF TSD algorithm is efficient for application to steady or unsteady transonic flow problems. It can provide accurate solutions in only several hundred time steps to yield a significant computational cost savings compared with alternative methods. This paper describes details of the governing flow equations and boundary conditions, with an emphasis on documenting the finite-difference formulas of the AF algorithm that were not reported in references 3 and 4.

## Symbols

$A$	coefficient in TSD equation (see eqs. (3))
$B$	coefficient in TSD equation (see eqs. (3))
$C$	coefficient in nonreflecting far-field boundary conditions (see eq. (14a))
$C_a$	angle-of-attack correction for bodies (see eqs. (12a) and (12b))
$C_p$	pressure coefficient
$C_{p_i}$	isentropic pressure coefficient
$C_{p_s}$	pressure coefficient due to change in entropy
$C_{p_v}$	pressure coefficient due to vorticity
$C_t$	thickness correction for bodies (see eqs. (12a) and (12b))
$c_v$	specific heat at constant volume
$D$	coefficient in nonreflecting far-field boundary conditions (see eq. (14b))
$E$	coefficient in TSD equation (see eqs. (3))
$F$	coefficient in TSD equation (see eqs. (4) to (7))
$F_1$	flux in $L_\xi$ operator (see eqs. (69) and (70))

$F_2$	flux in $L_\eta$ operator (see eq. (95))
$F_3$	flux in $L_\zeta$ operator (see eq. (111))
$f_0$	flux in time derivative in TSD equation (see eq. (2a))
$f_1$	flux in $x$ -direction in TSD equation (see eq. (2b))
$f_2$	flux in $y$ -direction in TSD equation (see eq. (2c))
$f_3$	flux in $z$ -direction in TSD equation (see eq. (2d))
$G$	coefficient in TSD equation (see eqs. (4) to (7))
$g_0$	flux in time derivative in TSD equation (see eq. (132a))
$g_1$	flux in $\xi$ -direction in TSD equation (see eq. (132b))
$g_1^s$	sonic reference flux (see eqs. (144) and (146))
$g_2$	flux in $\eta$ -direction in TSD equation (see eq. (132c))
$g_3$	flux in $\zeta$ -direction in TSD equation (see eq. (132d))
$H$	coefficient in TSD equation (see eqs. (4) to (7))
$i$	index in $\xi$ - or $x$ -direction
$j$	index in $\eta$ - or $y$ -direction
$K_v$	$= \frac{1}{1+Q}$
$k$	index in $\zeta$ - or $z$ -direction
$L_\zeta$	differential operator in $\zeta$ -direction
$L_\eta$	differential operator in $\eta$ -direction
$L_\xi$	differential operator in $\xi$ -direction
$M_\infty$	free-stream Mach number
$N_x$	component of normal vector on body in $x$ -direction (see eq. (11))
$N_y$	component of normal vector on body in $y$ -direction (see eq. (11))
$N_z$	component of normal vector on body in $z$ -direction (see eq. (11))
NXT	number of grid points in $\xi$ -direction
NYT	number of grid points in $\eta$ -direction
NZT	number of grid points in $\zeta$ -direction
$n$	index denoting time level
$Q$	constant (see eq. (16a))
$R$	residual (see eq. (131))
$s$	local change in entropy from free-stream value
$t$	nondimensional time
$u_s$	shock speed
$u_1$	flow speed upstream of shock (see eq. (20))
$V$	speed term (see eq. (16c))



$V^s$	sonic reference speed (see eq. (16b))
$W$	defined in equation (84)
$x$	physical coordinate in streamwise direction
$y$	physical coordinate in spanwise direction
$z$	physical coordinate in vertical direction
$\alpha_b$	angle of attack of body
$\beta_b$	yaw angle of body
$\Gamma$	wake circulation
$\gamma$	ratio of specific heats
$\Delta t$	nondimensional time step
$\Delta t_1$	step size from time level $n$ to time level $n + 1$ (see eq. (65))
$\Delta t_2$	step size from time level $n - 1$ to time level $n$ (see eq. (66))
$\Delta t_3$	step size from time level $n - 2$ to time level $n - 1$ (see eq. (67))
$\zeta$	computational coordinate in vertical direction
$\eta$	computational coordinate in spanwise direction
$\xi$	computational coordinate in streamwise direction
$\sigma$	relaxation parameter (see eq. (31))
$\Phi$	potential function (see eq. (23))
$\phi$	disturbance velocity potential
$\bar{\phi}$	first intermediate disturbance velocity potential
$\underline{\phi}$	second intermediate disturbance velocity potential
$\phi_x$	disturbance velocity in $x$ -direction
$\phi_y$	disturbance velocity in $y$ -direction
$\phi_z$	disturbance velocity in $z$ -direction
$\Psi$	function representing stretching and rotating of vortex filaments associated with entropy variation (see eq. (23))

## Governing Equations

### TSD Equation

The flow is assumed to be governed by the general-frequency, modified, unsteady TSD potential equation, which may be written in conservation law form as

$$\frac{\partial f_0}{\partial t} + \frac{\partial f_1}{\partial x} + \frac{\partial f_2}{\partial y} + \frac{\partial f_3}{\partial z} = 0 \quad (1)$$

where

$$f_0 = -A\phi_t - B\phi_x \quad (2a)$$

$$f_1 = E\phi_x + F\phi_x^2 + G\phi_y^2 \quad (2b)$$

$$f_2 = \phi_y + H\phi_x\phi_y \quad (2c)$$

$$f_3 = \phi_z \quad (2d)$$

The coefficients  $A$ ,  $B$ , and  $E$  are defined as

$$A = M_\infty^2 \quad B = 2M_\infty^2 \quad \text{and} \quad E = 1 - M_\infty^2 \quad (3)$$

Several choices are available within CAP-TSD for the coefficients  $F$ ,  $G$ , and  $H$  depending upon the assumptions used in deriving the TSD equation. Briefly, the coefficients are referred to as “NASA Ames” coefficients when defined as

$$F = -\frac{1}{2}(\gamma + 1)M_\infty^2 \quad G = \frac{1}{2}(\gamma - 3)M_\infty^2 \quad H = -(\gamma - 1)M_\infty^2 \quad (4)$$

and are referred to as “NLR” coefficients when defined as

$$F = -\frac{1}{2} \left[ 3 - (2 - \gamma)M_\infty^2 \right] M_\infty^2 \quad G = -\frac{1}{2}M_\infty^2 \quad H = -M_\infty^2 \quad (5)$$

The “classic” coefficients are given by

$$F = -\frac{1}{2}(\gamma + 1)M_\infty^2 \quad G = 0 \quad H = 0 \quad (6)$$

and finally the coefficients for the linear equation are

$$F = G = H = 0 \quad (7)$$

### Coordinate Transformation

The unsteady transonic small-disturbance equation is solved numerically on a finite-difference grid in a computational coordinate system  $(\xi, \eta, \zeta)$ . The finite-difference grids in both the physical and computational domains are contained within rectangular boundaries and conform to the leading and trailing edges of the horizontal lifting surfaces. Regions in the physical domain are mapped into rectangular regions in the computational domain using shearing transformations. For simplicity, no shearing is performed in the vertical direction, so that pylons and vertical tails are approximated by rectangular surfaces. The shearing transformation may be written generally as

$$\xi = \xi(x, y) \quad \eta = y \quad \zeta = z \quad (8)$$

where  $\xi$ ,  $\eta$ , and  $\zeta$  are the nondimensional computational coordinates in the  $x$ -,  $y$ -, and  $z$ -directions, respectively. The TSD equation (eq. (1)) may then be expressed in computational coordinates as

$$\begin{aligned} -\frac{\partial}{\partial t} \left( \frac{A}{\xi_x} \phi_t + B \phi_\xi \right) + \frac{\partial}{\partial \xi} \left[ E \xi_x \phi_\xi + F \xi_x^2 \phi_\xi^2 + G (\xi_y \phi_\xi + \phi_\eta)^2 + \frac{\xi_y}{\xi_x} (\xi_y \phi_\xi + \phi_\eta) + H \xi_y \phi_\xi (\xi_y \phi_\xi + \phi_\eta) \right] \\ + \frac{\partial}{\partial \eta} \left[ \frac{1}{\xi_x} (\xi_y \phi_\xi + \phi_\eta) + H \phi_\xi (\xi_y \phi_\xi + \phi_\eta) \right] + \frac{\partial}{\partial \zeta} \left( \frac{1}{\xi_x} \phi_\zeta \right) = 0 \end{aligned} \quad (9)$$

### Boundary Conditions

The horizontal lifting surfaces are modeled (ref. 6) by imposing the following boundary conditions.

Flow tangency:

$$\phi_z^\pm = f_x^\pm + f_t \quad (10a)$$

Trailing wake:

$$[\phi_z] = 0 \quad (10b)$$

$$[\phi_x + \phi_t] = 0 \quad (10c)$$

where  $f$  is a function describing the position of the lifting surface (including thickness, camber, angle of attack, yaw angle, and dihedral) and  $[\ ]$  indicates the jump in the indicated quantity across the wake. The flow-tangency condition is imposed along the mean plane of the respective lifting surface. In equation (10a), the plus and minus superscripts indicate the upper and lower surfaces of the mean plane, respectively. The wakes are assumed to be flat and horizontal.

Bodies such as the fuselage, stores, and nacelles are treated as follows. For a body at angle of attack  $\alpha_b$  and at yaw angle  $\beta_b$ , the exact steady flow-tangency boundary condition may be written as

$$N_x(1 + \phi_x) + N_y(\phi_y + \beta_b) + N_z(\phi_z + \alpha_b) = 0 \quad (11)$$

where  $N(x, y, z, t) = 0$  defines the body surface. Computationally, bodies are modeled with simplified boundary conditions applied on a computational box that extends to the upstream and downstream boundaries of the grid with a rectangular cross section rather than on the true surface (refs. 7 and 8.) The method is consistent with the small-disturbance approximation and treats bodies with sufficient accuracy to obtain the correct global effect on the flow field without the use of special grids or complicated coordinate transformations. As such, the approximations to the flow-tangency boundary condition (eq. (11)) imposed on the computational box are

$$\phi_y^\pm = -C_t \left( \frac{N_x}{N_y} \right)^\pm - C_a \beta_b \quad (12a)$$

for right or left surfaces and

$$\phi_z^\pm = -C_t \left( \frac{N_x}{N_z} \right)^\pm - C_a \alpha_b \quad (12b)$$

for top or bottom surfaces. The parameters  $C_t$  and  $C_a$  are thickness and angle-of-attack corrections, respectively, derived from slender-body theory to account for spatial differences between true and computational body surfaces (refs. 7 and 8.) Also, in equation (12a), the plus and minus superscripts indicate the right and left surfaces, respectively. In equation (12b), the plus and minus superscripts indicate the top and bottom surfaces, respectively.

The conditions imposed upon the outer boundary of the computational region are similar to the characteristic or “nonreflecting” boundary conditions reported by Whitlow (ref. 9.) The conditions employed here are given by the following.

Upstream:

$$\phi = 0 \quad (13a)$$

Downstream:

$$\frac{1}{2} \left( \frac{-B}{C} + \frac{D}{\sqrt{C}} \right) \phi_t + \phi_x = 0 \quad (13b)$$

Above:

$$\frac{D}{2} \phi_t + \phi_z = 0 \quad (13c)$$

Below:

$$\frac{D}{2} \phi_t - \phi_z = 0 \quad (13d)$$

Right spanwise:

$$\frac{D}{2}\phi_t + \phi_y = 0 \quad (13e)$$

Left spanwise (for full-span modeling):

$$\frac{D}{2}\phi_t - \phi_y = 0 \quad (13f)$$

Symmetry plane (for half-span modeling):

$$\phi_y = 0 \quad (13g)$$

where

$$C = E + 2F\phi_x \quad (14a)$$

$$D = \left(4A + \frac{B^2}{C}\right)^{1/2} \quad (14b)$$

### Entropy Model

An entropy model was developed for the AF algorithm (ref. 10), similar to that of reference 11, that includes (1) an alternative streamwise flux, (2) an entropy correction in the pressure formula, and (3) a modified wake boundary condition to account for convection of entropy. In this section, the entropy model is described.

**Alternative streamwise flux.** The entropy model is formulated by first replacing the streamwise flux  $f_1$  (eq. (2b)) in the TSD equation with an alternative flux given by

$$f_1 = (\gamma + 1)M_\infty^2 Q \left( VV^s - \frac{1}{2}V^2 \right) + G\phi_y^2 \quad (15)$$

where

$$Q = \left[ \frac{2 + (\gamma - 1)M_\infty^2}{(\gamma + 1)M_\infty^2} \right]^{1/2} \quad (16a)$$

$$V^s = \frac{Q^2 - 1}{2Q} \quad (16b)$$

$$V = \frac{(1 + Q)\phi_x}{1 + \phi_x + Q} \quad (16c)$$

**Pressure correction.** The pressure formula is modified to include entropy effects according to

$$C_p = C_{p_i} + C_{p_s} \quad (17)$$

where  $C_{p_i}$  is the isentropic pressure coefficient and  $C_{p_s}$  is the pressure coefficient due to the change in entropy. As reported in reference 10,  $C_{p_s}$  is given by

$$C_{p_s} = \frac{-2}{\gamma(\gamma - 1)M_\infty^2} \frac{s}{c_v} \quad (18)$$

where  $s$  is the change in entropy from the free-stream value. Equation (18) obviously requires the determination of entropy along the surface of the geometry being considered. This first requires the determination of shock location and then the calculation of the entropy jump across the shock. The shock location is easily determined since most TSD algorithms use type-dependent switching to capture shocks and to properly treat regions of subsonic and supersonic flow. The entropy jump is computed with the Rankine-Hugoniot shock jump relation:

$$\frac{s}{c_v} = \ln \frac{(\gamma + 1)u_1^2 - (\gamma - 1)Q^2}{(\gamma + 1)Q^2 - (\gamma - 1)u_1^2} - \gamma \ln \frac{u_1^2}{Q^2} \quad (19)$$

where

$$u_1 = 1 + \phi_x - u_s \quad (20)$$

In equation (20),  $u_1$  is the flow speed upstream of the shock and  $u_s$  is the shock speed. In the present formulation, the entropy is convected downstream from the shock according to

$$\frac{\partial s}{\partial t} + \frac{\partial s}{\partial x} = 0 \quad (21)$$

The correction to the pressure formula to include entropy effects (eq. (17)) does not directly affect the flow field. The effect on the flow field is produced by the modified wake boundary condition.

**Modified wake boundary condition.** The wake boundary condition requires that the pressure be continuous across the wake. Since the pressure formula (eq. (17)) includes a term due to entropy, the wake boundary condition must be similarly modified as

$$\Gamma_t + \Gamma_x = \frac{1}{2} \Delta C_{p_s} \quad (22)$$

where  $\Delta$  represents the jump across the wake. In equation (22),  $\Delta C_{p_s}$  is determined by first convecting the entropy along the wake and then computing  $C_{p_s}$  with equation (18). The nonzero right-hand side of equation (22) thus modifies the circulation distribution  $\Gamma$ .

### Vorticity Model

A vorticity model was developed for the AF algorithm (ref. 10) similar to that of reference 12. In this section, the vorticity model is described in detail, including (1) a modified velocity vector that in turn modifies the TSD equation, (2) a pressure formula correction for vorticity effects, and (3) the resulting wake boundary conditions.

**Modified velocity vector.** The vorticity model is formulated by first writing the velocity vector as the sum of potential and rotational parts according to

$$U = \nabla \Phi - \frac{1}{\gamma - 1} \frac{s}{c_v} \nabla \Psi \quad (23)$$

In equation (23), the first term is the gradient of a scalar potential  $\Phi$  and the second term is the product of the change in entropy  $s$  and the gradient of the function  $\Psi$ . The function  $\Psi$  is a measure of the stretching and rotating of vortex filaments associated with entropy variation (ref. 12). In the present algorithm, the rotational part of the velocity vector is assumed to occur only in the region downstream of shocks. Further assuming that the entropy convects with the free stream and that the shock curvature is negligible implies that

$$\frac{\partial \Psi}{\partial x} = \frac{1}{\gamma M_\infty^2} \quad \frac{\partial \Psi}{\partial y} = 0 \quad \frac{\partial \Psi}{\partial z} = 0 \quad (24)$$

These assumptions eliminate the variable  $\Psi$  from the model and leave only the change in entropy to be determined throughout the flow field. In a steady flow, entropy is constant along streamlines and changes only through shock waves. The entropy jump is computed along shocks with the Rankine-Hugoniot relation (eq. (19)). Then, for simplicity, the grid lines are assumed to approximate the streamlines of the flow, which is consistent with the small-disturbance approximation. The entropy is then convected downstream along the grid lines for unsteady applications (eq. (21)) or is held constant along the grid lines for steady applications.

The modified velocity vector in turn modifies the TSD equation because the streamwise disturbance speed  $u = \phi_x$  is now given by

$$u = \phi_x - \frac{1}{\gamma(\gamma - 1)M_\infty^2} \frac{s}{c_v} \quad (25)$$

The new TSD equation has the same conservation law form as equation (1), with new fluxes defined by simply replacing  $\phi_x$  by the modified speed given in equation (25).

**Pressure correction.** The pressure formula must also be modified when vorticity effects are included in the model. In general form, the pressure coefficient may be computed from

$$C_p = C_{p_i} + C_{p_s} + C_{p_v} \quad (26)$$

where  $C_{p_v}$  is the pressure coefficient correction due to vorticity. The correction due to vorticity approximately cancels the correction due to entropy, and thus the pressure coefficient  $C_p$  is given by the isentropic formula. At the TSD equation level, this is clearly demonstrated by first considering the general form of equation (17). Assuming the first-order small-disturbance pressure formula for  $C_{p_i}$ , defining  $C_{p_s}$  as given by equation (18), and replacing  $\phi_x$  by the modified disturbance speed of equation (25) yields

$$C_p = -2\phi_t - 2\phi_x - \frac{2}{\gamma(\gamma - 1)M_\infty^2} \frac{s}{c_v} + \frac{2}{\gamma(\gamma - 1)M_\infty^2} \frac{s}{c_v} \quad (27)$$

Here the corrections due to entropy and vorticity identically cancel each other, and thus the pressure coefficient is given by the isentropic formula in terms of the irrotational disturbance speed  $\phi_x$ .

**Modified wake boundary condition.** As with the entropy model, the wake boundary condition in the vorticity model requires that the pressure be continuous across the wake. Since the pressure is now given by the isentropic formula (eq. (27)), the wake boundary condition is identical to the original condition given by

$$\Gamma_t + \Gamma_x = 0 \quad (28)$$

Consequently, the modifications that are required when both entropy and vorticity effects are included are the alternative streamwise flux given by equation (15) and the modified streamwise disturbance speed given by equation (25).

## Approximate-Factorization Algorithm

### General Description

The AF algorithm consists of a time-linearization procedure coupled with a subiteration technique. For unsteady flow calculations, the solution procedure involves two steps. First, a time-linearization step (described below) is performed to determine an estimate of the potential field.

Second, subiterations are performed to minimize linearization and factorization errors. Specifically, the TSD equation is written in general form as

$$R(\phi^{n+1}) = 0 \quad (29)$$

where  $\phi^{n+1}$  represents the unknown potential field at time level  $n+1$ . The solution to equation (29) is then given by the linearization of equation (29) about  $\phi^*$ :

$$R(\phi^*) + \left( \frac{\partial R}{\partial \phi} \right)_{\phi=\phi^*} \Delta\phi = 0 \quad (30)$$

In equation (30),  $\phi^*$  is the currently available value of  $\phi^{n+1}$  and  $\Delta\phi = \phi^{n+1} - \phi^*$ . During convergence of the iteration procedure,  $\Delta\phi$  approaches zero so that the solution is given by  $\phi^{n+1} = \phi^*$ . In general, only one or two iterations at a given time level are required to achieve acceptable convergence. For steady flow calculations, iterations are not used since time accuracy is not necessary when marching to steady state.

### Mathematical Formulation

The AF algorithm is formulated by first approximating the time derivative terms ( $\phi_{tt}$  and  $\phi_{xt}$ ) by second-order-accurate finite-difference formulas. The TSD equation is rewritten by substituting  $\phi = \phi^* + \Delta\phi$  and neglecting squares of derivatives of  $\Delta\phi$ , which is equivalent to applying equation (30) term by term. The resulting equation is then rearranged and the left-hand side is approximately factored into a triple product of operators yielding

$$L_\xi L_\eta L_\zeta \Delta\phi = -\sigma R(\phi^*, \phi^n, \phi^{n-1}, \phi^{n-2}) \quad (31)$$

where the  $L_\xi$ ,  $L_\eta$ , and  $L_\zeta$  operators and the residual  $R$  are defined and described in subsequent sections. In equation (31)  $\sigma$  is a relaxation parameter that is normally set equal to 1.0. To accelerate convergence to steady state, the residual may be overrelaxed using  $\sigma > 1$ . Equation (31) is solved with three sweeps through the grid by sequentially applying the operators as follows.

$\xi$ -sweep:

$$L_\xi \Delta\bar{\phi} = -\sigma R \quad (32a)$$

$\eta$ -sweep:

$$L_\eta \Delta\bar{\bar{\phi}} = \Delta\bar{\phi} \quad (32b)$$

$\zeta$ -sweep:

$$L_\zeta \Delta\phi = \Delta\bar{\bar{\phi}} \quad (32c)$$

### Time-Linearization Step

An initial estimate of the potentials at time level  $n+1$  is required to start the subiteration process. This estimate is provided by performing a time-linearization calculation. The equations governing the time-linearization step are derived in a similar fashion as the equations for subiteration. The only difference is that the equations are formulated by linearizing about time level  $n$  rather than about the iteration level. This is accomplished by substituting  $\phi = \phi^n + \Delta\phi$  into the TSD equation (eq. (1)) and neglecting squares of derivatives of  $\Delta\phi$ , as done previously.

### Difference Equations for the Disturbance Velocity

The AF algorithm is simplified greatly, both mathematically and numerically, by first determining the disturbance velocity components  $\phi_x^*$ ,  $\phi_y^*$ , and  $\phi_z^*$ . These components are required in numerous

places throughout the AF solution procedure at the half-node points  $(i \pm 1/2, j, k)$ ,  $(i, j \pm 1/2, k)$ , and  $(i, j, k \pm 1/2)$ . The finite-difference formulas that approximate the velocity components are presented in this section. In these formulas the  $i, j$ , or  $k$  subscripts are often omitted for clarity. Also, the grid metrics that appear in the formulas are defined in the following section.

### At Half-Node Points $(i \pm 1/2, j, k)$

All the expressions for the velocity components are straightforward central-difference approximations that are centered at the half-node points to be consistent with the treatment of the fluxes in the AF algorithm. For example, at half-node points  $(i - 1/2, j, k)$ , the  $x$ - and  $y$ -components of the disturbance velocity are required. They are defined simply by

$$\phi_{x_{i-1/2,j}}^* = \xi_{x_{i-1/2,j}} \frac{\phi_i^* - \phi_{i-1}^*}{\xi_i - \xi_{i-1}} \quad (33)$$

$$\phi_{y_{i-1/2,j}}^* = \xi_{y_{i-1/2,j}} \frac{\phi_i^* - \phi_{i-1}^*}{\xi_i - \xi_{i-1}} + \frac{\phi_{i,j+1}^* - \phi_{i,j-1}^* + \phi_{i-1,j+1}^* - \phi_{i-1,j-1}^*}{2(\eta_{j+1} - \eta_{j-1})} \quad (34)$$

If vorticity effects are included, then the  $x$ -component is defined by

$$\phi_{x_{i-1/2,j}}^* = \xi_{x_{i-1/2,j}} \frac{\phi_i^* - \phi_{i-1}^*}{\xi_i - \xi_{i-1}} - \frac{1}{2\gamma(\gamma - 1)M_\infty^2} \left[ \left( \frac{s}{c_v} \right)_i^* + \left( \frac{s}{c_v} \right)_{i-1}^* \right] \quad (35)$$

Formulas for the components at  $(i + 1/2, j, k)$  are determined from equations (33) to (35) by incrementing the  $i$  index by one. Also, in the symmetry plane (normally taken to be  $j = 1$ ) the  $y$ -component of the disturbance velocity is set equal to zero to impose the symmetry condition (eq. (13g)). Namely,

$$\phi_{y_{i-1/2,j}}^* = 0 \quad (36)$$

Furthermore, the  $y$ -component of the disturbance velocity must be defined differently to account for the flow-tangency condition (eq. (12a)) for bodies. The side surface of the computational box that is used to model a body, for example, is located an equal distance between grid planes in the spanwise direction (i.e., between planes  $j$  and  $j - 1$ ). For grid points in the plane  $j$ , which is adjacent to the side surface, the  $y$ -component of the disturbance velocity is defined as the weighted average of values at  $j + 1/2$  (determined by finite differencing) and at  $j - 1/2$  (given by the boundary condition). The resulting formula is

$$\begin{aligned} \phi_{y_{i-1/2,j}}^* = & \frac{\eta_j - \eta_{j-1}}{\eta_{j+1} - \eta_{j-1}} \frac{1}{2} \left( \xi_{y_{i,j+1}} \frac{\phi_{i,j+1}^* - \phi_{i-1,j+1}^*}{\xi_i - \xi_{i-1}} + \xi_{y_{i,j}} \frac{\phi_{i,j}^* - \phi_{i-1,j}^*}{\xi_i - \xi_{i-1}} \right. \\ & \left. + \frac{\phi_{i,j+1}^* - \phi_{i,j}^*}{\eta_{j+1} - \eta_j} + \frac{\phi_{i-1,j+1}^* - \phi_{i-1,j}^*}{\eta_{j+1} - \eta_j} \right) \\ & - \frac{\eta_{j+1} - \eta_j}{\eta_{j+1} - \eta_{j-1}} \left[ C_{ti} \left( \frac{N_x}{N_y} \right)_i^+ + C_{a_i} \beta_b + C_{t_{i-1}} \left( \frac{N_x}{N_y} \right)_{i-1}^+ + C_{a_{i-1}} \beta_b \right] \end{aligned} \quad (37)$$

Similarly, for a full-span configuration, the  $y$ -component of the disturbance velocity is defined differently to treat the left side surface (located between planes  $j$  and  $j + 1$ ). Hence, for grid points in the plane  $j$  that is adjacent to the left side surface,



$$\begin{aligned}
\phi_{y_{i-1/2,j}}^* &= \frac{\eta_{j+1} - \eta_j}{\eta_{j+1} - \eta_{j-1}} \frac{1}{2} \left( \xi_{y_{i,j}} \frac{\phi_{i,j}^* - \phi_{i-1,j}^*}{\xi_i - \xi_{i-1}} + \xi_{y_{i,j-1}} \frac{\phi_{i,j-1}^* - \phi_{i-1,j-1}^*}{\xi_i - \xi_{i-1}} \right. \\
&\quad \left. + \frac{\phi_{i,j}^* - \phi_{i,j-1}^*}{\eta_j - \eta_{j-1}} + \frac{\phi_{i-1,j}^* - \phi_{i-1,j-1}^*}{\eta_j - \eta_{j-1}} \right) \\
&\quad - \frac{\eta_j - \eta_{j-1}}{\eta_{j+1} - \eta_{j-1}} \left[ C_{t_i} \left( \frac{N_x}{N_y} \right)_i^- + C_{a_i} \beta_b + C_{t_{i-1}} \left( \frac{N_x}{N_y} \right)_{i-1}^- + C_{a_{i-1}} \beta_b \right] \quad (38)
\end{aligned}$$

### At Half-Node Points ( $i, j \pm 1/2, k$ )

At half-node points ( $i, j - 1/2, k$ ) the  $x$ - and  $y$ -components are defined by

$$\phi_{x_{i,j-1/2}}^* = \xi_{x_{i,j-1/2}} \frac{\phi_{i+1,j}^* - \phi_{i-1,j}^* + \phi_{i+1,j-1}^* - \phi_{i-1,j-1}^*}{2(\xi_{i+1} - \xi_{i-1})} \quad (39)$$

$$\phi_{y_{i,j-1/2}}^* = \xi_{y_{i,j-1/2}} \frac{\phi_{i+1,j}^* - \phi_{i-1,j}^* + \phi_{i+1,j-1}^* - \phi_{i-1,j-1}^*}{2(\xi_{i+1} - \xi_{i-1})} + \frac{\phi_{i,j}^* - \phi_{i,j-1}^*}{\eta_j - \eta_{j-1}} \quad (40)$$

If vorticity effects are included, then the  $x$ -component is defined by

$$\begin{aligned}
\phi_{x_{i,j-1/2}}^* &= \xi_{x_{i,j-1/2}} \frac{\phi_{i+1,j}^* - \phi_{i-1,j}^* + \phi_{i+1,j-1}^* - \phi_{i-1,j-1}^*}{2(\xi_{i+1} - \xi_{i-1})} \\
&\quad - \frac{1}{2\gamma(\gamma - 1)M_\infty^2} \left[ \left( \frac{s}{c_v} \right)_j^* + \left( \frac{s}{c_v} \right)_{j-1}^* \right] \quad (41)
\end{aligned}$$

Formulas for the components at ( $i, j + 1/2, k$ ) are determined from equations (39) to (41) by incrementing the  $j$  index by one. Also, the formulas need to be modified to again account for the symmetry condition ( $j = J$ ; normally taken to be  $J = 1$ ). At  $j = J$ , the  $x$ - and  $y$ -components become

$$\phi_{x_{i,J-1/2}}^* = \phi_{x_{i,J+1/2}}^* \quad (42)$$

$$\phi_{y_{i,J-1/2}}^* = -\phi_{y_{i,J+1/2}}^* \quad (43)$$

Furthermore, both the  $x$ - and  $y$ -components of the disturbance velocity must be defined differently to account for the flow-tangency condition (eq. (12a)) for bodies. For half-node points ( $i, j - 1/2, k$ ) that lie on the right side surface of the computational box, a one-sided formula is used for the  $x$ -component given by

$$\begin{aligned}
\phi_{x_{i,j-1/2}}^* &= \frac{1}{2} \left( \frac{\eta_{j+1} - \eta_{j-1}}{\eta_{j+1} - \eta_j} \xi_{x_{i,j}} \frac{\phi_{i+1,j}^* - \phi_{i-1,j}^*}{\xi_{i+1} - \xi_{i-1}} - \frac{\eta_j - \eta_{j-1}}{\eta_{j+1} - \eta_j} \xi_{x_{i,j+1}} \frac{\phi_{i+1,j+1}^* - \phi_{i-1,j+1}^*}{\xi_{i+1} - \xi_{i-1}} \right) \\
&\quad + \frac{1}{2} \xi_{x_{i,j}} \frac{\phi_{i+1,j}^* - \phi_{i-1,j}^*}{\xi_{i+1} - \xi_{i-1}} \quad (44)
\end{aligned}$$

and the boundary condition is used for the  $y$ -component given by

$$\phi_{y_{i,j-1/2}}^* = -C_{t_i} \left( \frac{N_x}{N_y} \right)_i^+ - C_{a_i} \beta_b \quad (45)$$

For a full-span configuration, similar changes are required. For half-node points  $(i, j+1/2, k)$  that lie on the left side surface of the computational box,

$$\begin{aligned}\phi_{x_{i,j+1/2}}^* &= \frac{1}{2} \left( \frac{\eta_{j+1} - \eta_{j-1}}{\eta_j - \eta_{j-1}} \xi_{x_{i,j}} \frac{\phi_{i+1,j}^* - \phi_{i-1,j}^*}{\xi_{i+1} - \xi_{i-1}} - \frac{\eta_{j+1} - \eta_j}{\eta_j - \eta_{j-1}} \xi_{x_{i,j-1}} \frac{\phi_{i+1,j-1}^* - \phi_{i-1,j-1}^*}{\xi_{i+1} - \xi_{i-1}} \right) \\ &\quad + \frac{1}{2} \xi_{x_{i,j}} \frac{\phi_{i+1,j}^* - \phi_{i-1,j}^*}{\xi_{i+1} - \xi_{i-1}}\end{aligned}\quad (46)$$

$$\phi_{y_{i,j+1/2}}^* = -C_{t_i} \left( \frac{N_x}{N_y} \right)_i^- - C_{a_i} \beta_b \quad (47)$$

#### At Half-Node Points $(i, j, k \pm 1/2)$

At half-node points  $(i, j, k-1/2)$  only the  $z$ -component of the disturbance velocity is required. It is defined simply by

$$\phi_{z_{k-1/2}}^* = \frac{\phi_{i,k}^* - \phi_{i,k-1}^*}{\zeta_k - \zeta_{k-1}} \quad (48)$$

The formula for the  $z$ -component at  $(i, j, k+1/2)$  is determined from equation (48) by incrementing the  $k$  index by one. The  $z$ -component of the disturbance velocity, however, needs to be defined differently to account for the lifting-surface flow-tangency and wake boundary conditions. The lifting surfaces are located an equal distance between grid lines so that in the plane directly above the surface the  $\phi_{z_{k-1/2}}^*$  formula of equation (48) is replaced by  $(f_x^+ + f_t)^{n+1}$  and in the plane below the surface the  $\phi_{z_{k+1/2}}^*$  formula similar to that of equation (48) is replaced by  $(f_x^- + f_t)^{n+1}$ . For the wake boundary condition the solution procedure is modified by requiring that the disturbance velocity in the vertical direction be continuous across the wake (eq. (10b)). This condition is imposed by defining

$$\phi_{z_{k-1/2}}^* = \frac{\phi_k^* - (\phi_{k-1}^* - \Gamma^*)}{\zeta_k - \zeta_{k-1}} \quad (49)$$

at the grid points in the plane above the wake and by defining

$$\phi_{z_{k+1/2}}^* = \frac{(\phi_{k+1}^* - \Gamma^*) - \phi_k^*}{\zeta_{k+1} - \zeta_k} \quad (50)$$

at grid points in the plane below the wake. Furthermore, the  $z$ -component of the disturbance velocity must be defined differently to account for the flow-tangency boundary condition (eq. (12b)) for bodies. The top surface of the computational box that is used to model a body, for example, is located equidistantly between grid planes in the vertical direction (i.e., between planes  $k$  and  $k-1$ ). Hence, for grid points in the plane  $k$  that is above the top surface,

$$\phi_{z_{k-1/2}}^* = -C_{t_i} \left( \frac{N_x}{N_z} \right)_i^+ - C_{a_i} \alpha_b \quad (51)$$

Similarly, the bottom surface of the computational box is located equidistantly between grid planes in the vertical direction (i.e., between planes  $k$  and  $k+1$ ). Hence, for grid points in the plane  $k$  that is below the bottom surface,

$$\phi_{z_{k+1/2}}^* = -C_{t_i} \left( \frac{N_x}{N_z} \right)_i^- - C_{a_i} \alpha_b \quad (52)$$

## Difference Equations for the Grid Metrics

The finite-difference equations for the grid metrics are presented in this section. These equations were derived to be consistent with the differencing of the disturbance potentials, such that if the AF algorithm were a full-potential solver rather than a TSD solver, a uniform flow would be an exact result of the finite-difference formulas for the velocity components (presented in the previous section). The grid metrics are required in numerous places throughout the AF solution procedure at grid points  $(i, j, k)$  and at the half-node points  $(i \pm 1/2, j, k)$  and  $(i, j \pm 1/2, k)$ .

### At Grid Points $(i, j, k)$

At grid points  $(i, j, k)$ , the metrics are defined to be

$$\xi_{x_{i,j}} = \frac{\xi_{i+1} - \xi_{i-1}}{x_{i+1,j} - x_{i-1,j}} \quad (53)$$

$$\xi_{y_{i,j}} = -\frac{\xi_{i+1} - \xi_{i-1}}{x_{i+1,j} - x_{i-1,j}} \frac{x_{i,j+1} - x_{i,j-1}}{\eta_{j+1} - \eta_{j-1}} \quad (54)$$

However, at the upstream ( $i = 1$ ) and downstream ( $i = \text{NXT}$ ) boundaries of the grid,

$$\xi_{x_{i,j}} = 1 \quad (55)$$

$$\xi_{y_{i,j}} = 0 \quad (56)$$

Along the symmetry plane ( $j = 1$ ),

$$\xi_{y_{i,j}} = -\frac{\xi_{i+1} - \xi_{i-1}}{x_{i+1,j} - x_{i-1,j}} \frac{x_{i,j+1} - x_{i,j}}{\eta_{j+1} - \eta_j} \quad (57)$$

and along the far-spanwise boundary ( $j = \text{NYT}$ ),

$$\xi_{y_{i,j}} = -\frac{\xi_{i+1} - \xi_{i-1}}{x_{i+1,j} - x_{i-1,j}} \frac{x_{i,j} - x_{i,j-1}}{\eta_j - \eta_{j-1}} \quad (58)$$

### At Half-Node Points $(i \pm 1/2, j, k)$

At the half-node points  $(i - 1/2, j, k)$  the metrics are defined to be

$$\xi_{x_{i-1/2,j}} = \frac{\xi_i - \xi_{i-1}}{x_{i,j} - x_{i-1,j}} \quad (59)$$

$$\xi_{y_{i-1/2,j}} = -\frac{\xi_i - \xi_{i-1}}{x_{i,j} - x_{i-1,j}} \frac{x_{i,j+1} - x_{i,j-1} + x_{i-1,j+1} - x_{i-1,j-1}}{2(\eta_{j+1} - \eta_{j-1})} \quad (60)$$

However, along the symmetry plane ( $j = 1$ ),

$$\xi_{y_{i-1/2,j}} = -\frac{\xi_i - \xi_{i-1}}{x_{i,j} - x_{i-1,j}} \frac{x_{i,j+1} - x_{i,j} + x_{i-1,j+1} - x_{i-1,j}}{2(\eta_{j+1} - \eta_j)} \quad (61)$$

and along the far-spanwise boundary ( $j = \text{NYT}$ ),

$$\xi_{y_{i-1/2,j}} = -\frac{\xi_i - \xi_{i-1}}{x_{i,j} - x_{i-1,j}} \frac{x_{i,j} - x_{i,j-1} + x_{i-1,j} - x_{i-1,j-1}}{2(\eta_j - \eta_{j-1})} \quad (62)$$

### At Half-Node Points ( $i, j \pm 1/2, k$ )

At half-node points ( $i, j \pm 1/2, k$ ), the metrics are defined to be

$$\xi_{x_{i,j-1/2}} = \frac{2(\xi_{i+1} - \xi_{i-1})}{x_{i+1,j} - x_{i-1,j} + x_{i+1,j-1} + x_{i-1,j-1}} \quad (63)$$

$$\xi_{y_{i,j-1/2}} = \frac{-2(\xi_{i+1} - \xi_{i-1})}{x_{i+1,j} - x_{i-1,j} + x_{i+1,j-1} + x_{i-1,j-1}} \frac{x_{i,j} - x_{i,j-1}}{\eta_j - \eta_{j-1}} \quad (64)$$

## Difference Equations for the Left-Hand-Side Operators

The finite-difference equations for the  $L_\xi$ ,  $L_\eta$ , and  $L_\zeta$  operators are presented in this section, including the modifications that are required to impose the symmetry plane, lifting-surface flow-tangency, and wake boundary conditions and the flow-tangency conditions for bodies. Also, the time derivatives in the AF algorithm have been written for variable time stepping to allow for step-size cycling to accelerate convergence to steady state. Because of this, three different time steps are required as defined by

$$\Delta t_1 = t^{n+1} - t^n \quad (65)$$

$$\Delta t_2 = t^n - t^{n-1} \quad (66)$$

$$\Delta t_3 = t^{n-1} - t^{n-2} \quad (67)$$

### $L_\xi$ Operator

The  $L_\xi$  operator is implemented by considering the  $\xi$ -sweep equation defined by

$$L_\xi \Delta \bar{\phi} = \left( 1 + \frac{B}{2A} \frac{2 \Delta t_1 + \Delta t_2}{\Delta t_1 + \Delta t_2} \Delta t_2 \xi_x \frac{\partial}{\partial \xi} - \frac{\Delta t_1 \Delta t_2}{2A} \xi_x \frac{\partial}{\partial \xi} F_1 \frac{\partial}{\partial \xi} \right) \Delta \bar{\phi} = -R \quad (68)$$

where, for the isentropic formulation,

$$F_1 = E\xi_x + 2F\xi_x\phi_x^* + 2G\xi_y\phi_y^* + \frac{\xi_y^2}{\xi_x} (1 + H\phi_x^*) + H\xi_y\phi_y^* \quad (69)$$

for the nonisentropic formulation,

$$F_1 = \xi_x(\gamma + 1)M_\infty^2 QW (V^s - V) (1 - K_v V) + 2G\xi_y\phi_y^* + \frac{\xi_y^2}{\xi_x} (1 + H\phi_x^*) + H\xi_y\phi_y^* \quad (70)$$

and  $R$  is the residual, which is treated in a subsequent section. The first derivative in the  $L_\xi$  operator is represented by a backward-difference formula, to maintain numerical stability, given by

$$\frac{\partial}{\partial \xi} (\Delta \bar{\phi}) = \frac{2}{\xi_{i+1} - \xi_{i-1}} (\Delta \bar{\phi}_i - \Delta \bar{\phi}_{i-1}) \quad (71)$$

The other derivative in the  $L_\xi$  operator is treated by first considering the flux  $F_1$  as being the sum of two fluxes, so that

$$\frac{\partial}{\partial \xi} F_1 \frac{\partial}{\partial \xi} (\Delta \bar{\phi}) = \frac{\partial}{\partial \xi} F_1^{\text{EO}} \frac{\partial}{\partial \xi} (\Delta \bar{\phi}) + \frac{\partial}{\partial \xi} F_1^{\text{CD}} \frac{\partial}{\partial \xi} (\Delta \bar{\phi}) \quad (72)$$

where

$$F_1^{\text{CD}} = (2G + H)\xi_y\phi_y^* + \frac{\xi_y^2}{\xi_x}(1 + H\phi_x^*) \quad (73)$$

and  $F_1^{\text{EO}}$  is taken to be one of two different formulas depending upon whether entropy effects are included. For example, in the original isentropic formulation,

$$F_1^{\text{EO}} = E\xi_x + 2F\xi_x\phi_x^* \quad (74)$$

and in the nonisentropic formulation,

$$F_1^{\text{EO}} = \xi_x(\gamma + 1)M_\infty^2 QW(V^s - V)(1 - K_v V) \quad (75)$$

Regardless of which definition is selected,  $F_1^{\text{EO}}$  is either centrally differenced at subsonic points or backward differenced at supersonic points according to the Engquist-Osher (EO) type-dependent mixed-difference operator (ref. 13), and  $F_1^{\text{CD}}$  is always centrally differenced (CD) independent of the local speed of the flow. Specifically, the second derivative of the first flux is represented by the following EO type-dependent formula:

$$\begin{aligned} \frac{\partial}{\partial \xi} F_1^{\text{EO}} \frac{\partial}{\partial \xi} (\Delta \bar{\phi}) &= \frac{2}{\xi_{i+1} - \xi_{i-1}} \left[ (1 - \varepsilon_{i+1/2}) F_{1_{i+1/2}}^{\text{EO}} \frac{\Delta \bar{\phi}_{i+1} - \Delta \bar{\phi}_i}{\xi_{i+1} - \xi_i} \right. \\ &\quad \left. + (2\varepsilon_{i-1/2} - 1) F_{1_{i-1/2}}^{\text{EO}} \frac{\Delta \bar{\phi}_i - \Delta \bar{\phi}_{i-1}}{\xi_i - \xi_{i-1}} - \varepsilon_{i-3/2} F_{1_{i-3/2}}^{\text{EO}} \frac{\Delta \bar{\phi}_{i-1} - \Delta \bar{\phi}_{i-2}}{\xi_{i-1} - \xi_{i-2}} \right] \end{aligned} \quad (76)$$

where in the isentropic formulation,

$$F_{1_{i-1/2}}^{\text{EO}} = E\xi_{x_{i-1/2,j}} + 2F\xi_{x_{i-1/2,j}}\phi_{x_{i-1/2,j}}^* \quad (77)$$

$$\varepsilon_{i-1/2} = \begin{cases} 0 & (\phi_{x_{i-1/2,j}}^* \leq \phi_x^s) \\ 1 & (\phi_{x_{i-1/2,j}}^* > \phi_x^s) \end{cases} \quad (78a)$$

$$\quad (78b)$$

and the sonic streamwise speed  $\phi_x^s$  is defined by

$$\phi_x^s = \frac{-E}{2F} \quad (79)$$

In the nonisentropic formulation,

$$F_{1_{i-1/2}}^{\text{EO}} = \xi_{x_{i-1/2,j}}(\gamma + 1)M_\infty^2 QW_{i-1/2,j}(V^s - V_{i-1/2,j})(1 - K_v V_{i-1/2,j}) \quad (80)$$

$$\varepsilon_{i-1/2} = \begin{cases} 0 & (V_{i-1/2,j} \leq V^s) \\ 1 & (V_{i-1/2,j} > V^s) \end{cases} \quad (81a)$$

$$(81b)$$

$$V_{i-1/2,j} = \frac{\phi_{x_{i-1/2,j}}^*}{1 + K_v \phi_{x_{i-1/2,j}}^*} \quad (83)$$

$$W_{i-1/2,j} = \frac{1}{1 + K_v \phi_{x_{i-1/2,j}}^*} \quad (84)$$

Recall from equations (16a) and (16b) that

$$Q = \left[ \frac{2 + (\gamma - 1)M_\infty^2}{(\gamma + 1)M_\infty^2} \right]^{1/2}$$

$$V^s = \frac{Q^2 - 1}{2Q}$$

The derivative involving the second flux ( $F_1^{\text{CD}}$ ) is represented by a central-difference formula involving terms evaluated at the half-node points in the  $\xi$ -direction according to

$$\frac{\partial}{\partial \xi} F_1^{\text{CD}} \frac{\partial}{\partial \xi} (\Delta \bar{\phi}) = \frac{2}{\xi_{i+1} - \xi_{i-1}} \left( F_{1_{i+1/2}}^{\text{CD}} \frac{\Delta \bar{\phi}_{i+1} - \Delta \bar{\phi}_i}{\xi_{i+1} - \xi_i} - F_{1_{i-1/2}}^{\text{CD}} \frac{\Delta \bar{\phi}_i - \Delta \bar{\phi}_{i-1}}{\xi_i - \xi_{i-1}} \right) \quad (85)$$

where

$$F_{1_{i-1/2}}^{\text{CD}} = (2G + H)\xi_{y_{i-1/2,j}}\phi_{y_{i-1/2,j}}^* + \frac{\xi_{y_{i-1/2,j}}}{\xi_{x_{i-1/2,j}}} \left( 1 + H\phi_{x_{i-1/2,j}}^* \right) \quad (86)$$

The derivative involving the second flux at the symmetry plane (normally taken to be  $j = 1$ ), however, needs to be defined differently to impose the symmetry condition. This results from requiring that

$$\phi_{y_{i-1/2,j}}^* = 0 \quad (87)$$

which implies that

$$\frac{\partial}{\partial \xi} F_1^{\text{CD}} \frac{\partial}{\partial \xi} (\Delta \bar{\phi}) = 0 \quad (88)$$

for grid points in the symmetry plane.

The  $\xi$ -sweep equation may then be rewritten for solution in quadradiagonal form as

$$b_i \Delta \bar{\phi}_{i-2} + c_i \Delta \bar{\phi}_{i-1} + d_i \Delta \bar{\phi}_i + e_i \Delta \bar{\phi}_{i+1} = -R_i \quad (89)$$

where

$$b_i = \frac{-\Delta t_1 \Delta t_2}{2A} \xi_{x_{i,j}} \frac{2}{\xi_{i+1} - \xi_{i-1}} \frac{1}{\xi_{i-1} - \xi_{i-2}} \varepsilon_{i-3/2} F_{1_{i-3/2}}^{\text{EO}} \quad (90a)$$

$$\begin{aligned} c_i = & -\frac{B}{2A} \frac{2 \Delta t_1 + \Delta t_2}{\Delta t_1 + \Delta t_2} \Delta t_2 \xi_{x_{i,j}} \frac{2}{\xi_{i+1} - \xi_{i-1}} \\ & + \frac{\Delta t_1 \Delta t_2}{2A} \xi_{x_{i,j}} \frac{2}{\xi_{i+1} - \xi_{i-1}} \left[ \frac{1}{\xi_i - \xi_{i-1}} (2\varepsilon_{i-1/2} - 1) F_{1_{i-1/2}}^{\text{EO}} + \frac{1}{\xi_{i-1} - \xi_{i-2}} \varepsilon_{i-3/2} F_{1_{i-3/2}}^{\text{EO}} \right] \\ & - \frac{\Delta t_1 \Delta t_2}{2A} \xi_{x_{i,j}} \frac{2}{\xi_{i+1} - \xi_{i-1}} \frac{1}{\xi_i - \xi_{i-1}} F_{1_{i-1/2}}^{\text{CD}} \end{aligned} \quad (90b)$$

$$\begin{aligned} d_i = & 1 + \frac{B}{2A} \frac{2 \Delta t_1 + \Delta t_2}{\Delta t_1 + \Delta t_2} \Delta t_2 \xi_{x_{i,j}} \frac{2}{\xi_{i+1} - \xi_{i-1}} \\ & + \frac{\Delta t_1 \Delta t_2}{2A} \xi_{x_{i,j}} \frac{2}{\xi_{i+1} - \xi_{i-1}} \left[ \frac{1}{\xi_{i+1} - \xi_i} (1 - \varepsilon_{i+1/2}) F_{1_{i+1/2}}^{\text{EO}} - \frac{1}{\xi_i - \xi_{i-1}} (2\varepsilon_{i-1/2} - 1) F_{1_{i-1/2}}^{\text{EO}} \right] \\ & + \frac{\Delta t_1 \Delta t_2}{2A} \xi_{x_{i,j}} \frac{2}{\xi_{i+1} - \xi_{i-1}} \left[ \frac{1}{\xi_{i+1} - \xi_i} F_{1_{i+1/2}}^{\text{CD}} + \frac{1}{\xi_i - \xi_{i-1}} F_{1_{i-1/2}}^{\text{CD}} \right] \end{aligned} \quad (90c)$$

$$e_i = -\frac{\Delta t_1 \Delta t_2}{2A} \xi_{x_{i,j}} \frac{2}{\xi_{i+1} - \xi_{i-1}} \frac{1}{\xi_{i+1} - \xi_i} \left(1 - \varepsilon_{i+1/2}\right) F_{1_{i+1/2}}^{\text{EO}} - \frac{\Delta t_1 \Delta t_2}{2A} \xi_{x_{i,j}} \frac{2}{\xi_{i+1} - \xi_{i-1}} \frac{1}{\xi_{i+1} - \xi_i} F_{1_{i+1/2}}^{\text{CD}} \quad (90d)$$

Note that it is more efficient computationally to first calculate  $b_i$ ,  $c_i$ , and  $e_i$  and then evaluate the main diagonal according to

$$d_i = 1 - b_i - c_i - e_i \quad (91)$$

Also,  $b_i = 0$  for a purely subsonic flow, so that further computational efficiency may be obtained by using a tridiagonal inversion procedure to calculate  $\Delta \bar{\phi}$  rather than the more costly quadradiagonal procedure that is necessary for mixed subsonic-supersonic type flows.

Modifications to the  $L_\xi$  operator are required to accommodate the flow-tangency boundary conditions for bodies. For example, inside the computational box that is used to model a body there is, of course, no flow. Therefore, at grid points that lie inside,

$$\Delta \bar{\phi} = 0 \quad (92)$$

which results in the following quadradiagonal coefficients and residual (or right-hand side):

$$b_i = 0 \quad (93a)$$

$$c_i = 0 \quad (93b)$$

$$d_i = 1 \quad (93c)$$

$$e_i = 0 \quad (93d)$$

$$R_i = 0 \quad (93e)$$

### $L_\eta$ Operator

The  $L_\eta$  operator is implemented by considering the  $\eta$ -sweep equation defined by

$$L_\eta \Delta \bar{\phi} = \left(1 - \xi_x \frac{\Delta t_1 \Delta t_2}{2A} \frac{\partial}{\partial \eta} F_2 \frac{\partial}{\partial \eta}\right) \Delta \bar{\phi} = \Delta \bar{\phi} \quad (94)$$

where

$$F_2 = \frac{1}{\xi_x} (1 + H \phi_x^*) \quad (95)$$

The spatial derivative of the  $L_\eta$  operator is represented by a central-difference formula involving terms evaluated at the half-node points in the  $\eta$ -direction according to

$$\frac{\partial}{\partial \eta} F_2 \frac{\partial}{\partial \eta} (\Delta \bar{\phi}) = \frac{2}{\eta_{j+1} - \eta_{j-1}} \left( F_{2_{i,j+1/2}} \frac{\Delta \bar{\phi}_{j+1} - \Delta \bar{\phi}_j}{\eta_{j+1} - \eta_j} - F_{2_{i,j-1/2}} \frac{\Delta \bar{\phi}_j - \Delta \bar{\phi}_{j-1}}{\eta_j - \eta_{j-1}} \right) \quad (96)$$

where

$$F_{2_{i,j-1/2}} = \frac{1}{\xi_{x_{i,j-1/2}}} (1 + H \phi_{x_{i,j-1/2}}^*) \quad (97)$$

The  $\eta$ -sweep equation may then be rewritten for solution in tridiagonal form as

$$c_j \Delta \bar{\phi}_{j-1} + d_j \Delta \bar{\phi}_j + e_j \Delta \bar{\phi}_{j+1} = \Delta \bar{\phi} \quad (98)$$

where

$$c_j = -\xi_{x_{i,j}} \frac{\Delta t_1 \Delta t_2}{2A} \frac{2}{\eta_{j+1} - \eta_{j-1}} \frac{1}{\eta_j - \eta_{j-1}} F_{2_{i,j-1/2}} \quad (99a)$$

$$d_j = 1 + \xi_{x_{i,j}} \frac{\Delta t_1 \Delta t_2}{2A} \frac{2}{\eta_{j+1} - \eta_{j-1}} \frac{1}{\eta_{j+1} - \eta_j} F_{2_{i,j+1/2}} \\ + \xi_{x_{i,j}} \frac{\Delta t_1 \Delta t_2}{2A} \frac{2}{\eta_{j+1} - \eta_{j-1}} \frac{1}{\eta_j - \eta_{j-1}} F_{2_{i,j-1/2}} \quad (99b)$$

$$e_j = -\xi_{x_{i,j}} \frac{\Delta t_1 \Delta t_2}{2A} \frac{2}{\eta_{j+1} - \eta_{j-1}} \frac{1}{\eta_{j+1} - \eta_j} F_{2_{i,j+1/2}} \quad (99c)$$

Note that it is more efficient computationally to first calculate  $c_j$  and  $e_j$ , and then evaluate the main diagonal according to

$$d_j = 1 - c_j - e_j \quad (100)$$

A special  $L_\eta$  operator is defined to impose the symmetry condition ( $j = J$ ; normally taken to be  $J = 1$ ). This is accomplished by requiring that

$$\left[ F_2 \frac{\partial}{\partial \eta} (\Delta \bar{\bar{\phi}}) \right]_{J-1/2} = - \left[ F_2 \frac{\partial}{\partial \eta} (\Delta \bar{\bar{\phi}}) \right]_{J+1/2} \quad (101)$$

The spatial derivative of the  $L_\eta$  operator is then given by

$$\frac{\partial}{\partial \eta} F_2 \frac{\partial}{\partial \eta} (\Delta \bar{\bar{\phi}}) = \frac{2}{\eta_{J+1} - \eta_J} F_{2_{i,J+1/2}} \frac{\Delta \bar{\bar{\phi}}_{J+1} - \Delta \bar{\bar{\phi}}_J}{\eta_{J+1} - \eta_J} \quad (102)$$

which results in an upper bidiagonal  $\eta$ -sweep equation at the symmetry plane defined by

$$c_J = 0 \quad (103a)$$

$$d_J = 1 + \xi_{x_{i,j}} \frac{\Delta t_1 \Delta t_2}{2A} \frac{2}{(\eta_{J+1} - \eta_J)^2} F_{2_{i,j+1/2}} \quad (103b)$$

$$e_J = -\xi_{x_{i,j}} \frac{\Delta t_1 \Delta t_2}{2A} \frac{2}{(\eta_{J+1} - \eta_J)^2} F_{2_{i,j+1/2}} \quad (103c)$$

Modifications to the  $L_\eta$  operator, similar to the modifications made to the  $L_\xi$  operator, are also required to accommodate the flow-tangency boundary conditions for bodies. For grid points that lie inside the computational box that is used to model a body,

$$\Delta \bar{\bar{\phi}} = 0 \quad (104)$$

which results in the following tridiagonal coefficients and right-hand side:

$$c_j = 0 \quad (105a)$$

$$d_j = 1 \quad (105b)$$

$$e_j = 0 \quad (105c)$$

$$R_j = 0 \quad (105d)$$



For grid points in the plane  $j$  that is adjacent to the right side of the computational box to which the body boundary conditions are applied,

$$\frac{\partial}{\partial y} (\Delta \bar{\phi})_{j-1/2} = 0 \quad (106)$$

which results in the following tridiagonal coefficients:

$$c_j = 0 \quad (107a)$$

$$d_j = 1 + \xi_{x,i,j} \frac{\Delta t_1 \Delta t_2}{2A} \frac{2}{\eta_{j+1} - \eta_{j-1}} \frac{1}{\eta_{j+1} - \eta_j} F_{2,j+1/2} \quad (107b)$$

$$e_j = -\xi_{x,i,j} \frac{\Delta t_1 \Delta t_2}{2A} \frac{2}{\eta_{j+1} - \eta_{j-1}} \frac{1}{\eta_{j+1} - \eta_j} F_{2,j+1/2} \quad (107c)$$

For full-span configurations, a similar modification is required to treat the left side of the computational box. For grid points in the plane  $j$  that is adjacent to the left side,

$$\frac{\partial}{\partial y} (\Delta \bar{\phi})_{j+1/2} = 0 \quad (108)$$

which results in

$$c_j = -\xi_{x,i,j} \frac{\Delta t_1 \Delta t_2}{2A} \frac{2}{\eta_{j+1} - \eta_{j-1}} \frac{1}{\eta_j - \eta_{j-1}} F_{2,j-1/2} \quad (109a)$$

$$d_j = 1 + \xi_{x,i,j} \frac{\Delta t_1 \Delta t_2}{2A} \frac{2}{\eta_{j+1} - \eta_{j-1}} \frac{1}{\eta_j - \eta_{j-1}} F_{2,j-1/2} \quad (109b)$$

$$e_j = 0 \quad (109c)$$

### $L_\zeta$ Operator

The  $L_\zeta$  operator is implemented by considering the  $\zeta$ -sweep equation defined by

$$L_\zeta \Delta \phi = \left( 1 - \xi_x \frac{\Delta t_1 \Delta t_2}{2A} \frac{\partial}{\partial \zeta} F_3 \frac{\partial}{\partial \zeta} \right) \Delta \phi = \Delta \bar{\phi} \quad (110)$$

where

$$F_3 = \frac{1}{\xi_x} \quad (111)$$

In the present implementation of the AF algorithm, there is no grid shearing in the vertical direction. Consequently, the metric  $\xi_x$  is independent of the  $\zeta$ -direction, and the  $\xi_x$  in the numerator of the  $L_\zeta$  operator identically cancels the  $\xi_x$  in the denominator of  $F_3$ . The spatial derivative in the operator is thus represented quite simply as

$$\frac{\partial^2}{\partial \zeta^2} (\Delta \phi) = \frac{2}{\zeta_{k+1} - \zeta_{k-1}} \left[ \frac{\Delta \phi_{k+1} - \Delta \phi_k}{\zeta_{k+1} - \zeta_k} - \frac{\Delta \phi_k - \Delta \phi_{k-1}}{\zeta_k - \zeta_{k-1}} \right] \quad (112)$$

The  $\zeta$ -sweep equation may then be rewritten for solution in tridiagonal form as

$$c_k \Delta \phi_{k-1} + d_k \Delta \phi_k + e_k \Delta \phi_{k+1} = \Delta \bar{\phi} \quad (113)$$

where

$$c_k = -\frac{\Delta t_1 \Delta t_2}{2A} \frac{2}{\zeta_{k+1} - \zeta_{k-1}} \frac{1}{\zeta_k - \zeta_{k-1}} \quad (114a)$$

$$d_k = 1 + \frac{\Delta t_1 \Delta t_2}{2A} \frac{2}{\zeta_{k+1} - \zeta_{k-1}} \frac{1}{\zeta_{k+1} - \zeta_k} + \frac{\Delta t_1 \Delta t_2}{2A} \frac{2}{\zeta_{k+1} - \zeta_{k-1}} \frac{1}{\zeta_k - \zeta_{k-1}} \quad (114b)$$

$$e_k = -\frac{\Delta t_1 \Delta t_2}{2A} \frac{2}{\zeta_{k+1} - \zeta_{k-1}} \frac{1}{\zeta_{k+1} - \zeta_k} \quad (114c)$$

Again note that it is more efficient computationally to first calculate  $c_k$  and  $e_k$  and then evaluate the main diagonal according to

$$d_k = 1 - c_k - e_k \quad (115)$$

The  $L_\zeta$  operator, however, needs to be defined differently to account for the lifting-surface flow-tangency and wake boundary conditions. Further, the operator must be modified in both the time-linearization and the subiteration step. First consider the modification in the time-linearization step. The lifting surfaces are located equidistantly between grid lines so that in the plane directly above the surface the derivative in equation (112) represented by

$$\frac{\Delta \phi_k - \Delta \phi_{k-1}}{\zeta_k - \zeta_{k-1}}$$

is replaced by

$$\left(f_x^+ + f_t\right)^{n+1} - \left(f_x^+ + f_t\right)^n$$

and in the plane below the surface the derivative in equation (112) represented by

$$\frac{\Delta \phi_{k+1} - \Delta \phi_k}{\zeta_{k+1} - \zeta_k}$$

is replaced by

$$\left(f_x^- + f_t\right)^{n+1} - \left(f_x^- + f_t\right)^n$$

Since these new terms are known quantities, they are brought to the right-hand side of the  $\zeta$ -sweep equation to create bidiagonal equations. For example, for grid points in the plane above the surface the tridiagonal coefficients become

$$c_k = 0 \quad (116a)$$

$$d_k = 1 + \frac{\Delta t_1 \Delta t_2}{2A} \frac{2}{\zeta_{k+1} - \zeta_{k-1}} \frac{1}{\zeta_{k+1} - \zeta_k} \quad (116b)$$

$$e_k = -\frac{\Delta t_1 \Delta t_2}{2A} \frac{2}{\zeta_{k+1} - \zeta_{k-1}} \frac{1}{\zeta_{k+1} - \zeta_k} \quad (116c)$$

and the corresponding right-hand side of the  $\zeta$ -sweep equation is

$$\Delta \bar{\phi} - \frac{\Delta t_1 \Delta t_2}{2A} \frac{2}{\zeta_{k+1} - \zeta_{k-1}} \left[ \left(f_x^+ + f_t\right)^{n+1} - \left(f_x^+ + f_t\right)^n \right]$$

For grid points in the plane below the surface the tridiagonal coefficients become

$$c_k = -\frac{\Delta t_1 \Delta t_2}{2A} \frac{2}{\zeta_{k+1} - \zeta_{k-1}} \frac{1}{\zeta_k - \zeta_{k-1}} \quad (117a)$$

$$d_k = 1 + \frac{\Delta t_1 \Delta t_2}{2A} \frac{2}{\zeta_{k+1} - \zeta_{k-1}} \frac{1}{\zeta_k - \zeta_{k-1}} \quad (117b)$$

$$e_k = 0 \quad (117c)$$

and the corresponding right-hand side of the  $\zeta$ -sweep equation is

$$\Delta \bar{\bar{\phi}} - \frac{\Delta t_1 \Delta t_2}{2A} \frac{2}{\zeta_{k+1} - \zeta_{k-1}} \left[ (f_x^- + f_t)^{n+1} - (f_x^- + f_t)^n \right]$$

Now consider the modification in the subiteration step. Here, similar changes are made to replace the derivatives in equation (112) by the difference in downwash at time levels  $n+1$  and  $*$  for grid points in the planes above and below the lifting surface. This results in the same tridiagonal coefficients as derived in equations (116) and (117). However, the right-hand side of the  $\zeta$ -sweep equation remains simply  $\Delta \bar{\bar{\phi}}$  since

$$(f_x^+ + f_t)^* = (f_x^+ + f_t)^{n+1} \quad (118a)$$

$$(f_x^- + f_t)^* = (f_x^- + f_t)^{n+1} \quad (118b)$$

The  $L_\zeta$  operator is also modified to account for the wake boundary condition in a way similar to that for the flow-tangency condition. To accomplish this, the wake circulation  $\Gamma$  is first calculated from equation (10c), which is equivalent to

$$\Gamma_{x_{i-1/2}}^{n+1} + \Gamma_{t_{i-1/2}}^{n+1} = 0 \quad (119)$$

This equation is discretized with second-order-accurate finite-difference approximations for the space and time derivatives, which results in

$$\begin{aligned} \xi_{x_{i-1/2,j}} \frac{\Gamma_i^{n+1} - \Gamma_{i-1}^{n+1}}{\xi_i - \xi_{i-1}} + \frac{1}{2} \left( \frac{2 \Delta t_1 + \Delta t_2}{\Delta t_1 + \Delta t_2} \frac{\Gamma_i^{n+1} - \Gamma_i^n}{\Delta t_1} - \frac{\Delta t_1}{\Delta t_1 + \Delta t_2} \frac{\Gamma_i^n - \Gamma_i^{n-1}}{\Delta t_2} \right. \\ \left. + \frac{2 \Delta t_1 + \Delta t_2}{\Delta t_1 + \Delta t_2} \frac{\Gamma_i^{n+1} - \Gamma_{i-1}^n}{\Delta t_1} - \frac{\Delta t_1}{\Delta t_1 + \Delta t_2} \frac{\Gamma_{i-1}^n - \Gamma_{i-1}^{n-1}}{\Delta t_2} \right) = 0 \end{aligned} \quad (120)$$

The equation is solved for the unknown circulation  $\Gamma_i^{n+1}$ , which yields

$$\begin{aligned} \Gamma_i^{n+1} = \left( \xi_{x_{i-1/2,j}} \frac{1}{\xi_i - \xi_{i-1}} + \frac{1}{2} \frac{2 \Delta t_1 + \Delta t_2}{\Delta t_1 + \Delta t_2} \frac{1}{\Delta t_1} \right)^{-1} \left[ \xi_{x_{i-1/2,j}} \frac{\Gamma_{i-1}^{n+1}}{\xi_i - \xi_{i-1}} \right. \\ \left. + \frac{1}{2} \left( - \frac{2 \Delta t_1 + \Delta t_2}{\Delta t_1 + \Delta t_2} \frac{\Gamma_i^n}{\Delta t_1} - \frac{\Delta t_1}{\Delta t_1 + \Delta t_2} \frac{\Gamma_i^n - \Gamma_i^{n-1}}{\Delta t_2} \right. \right. \\ \left. \left. + \frac{2 \Delta t_1 + \Delta t_2}{\Delta t_1 + \Delta t_2} \frac{\Gamma_{i-1}^{n+1} - \Gamma_{i-1}^n}{\Delta t_1} - \frac{\Delta t_1}{\Delta t_1 + \Delta t_2} \frac{\Gamma_{i-1}^n - \Gamma_{i-1}^{n-1}}{\Delta t_2} \right) \right] \end{aligned} \quad (121)$$

Through use of equation (121), the circulation is convected downstream by calculating  $\Gamma_i^{n+1}$  for all grid points downstream of the trailing edge, beginning with the trailing-edge value  $\Gamma_{te} = \phi_{te}^+ - \phi_{te}^-$ . The wake circulation is then incorporated within the solution procedure by requiring that the

disturbance velocity in the vertical direction be continuous across the wake (eq. (10b)). This condition is imposed by defining

$$\frac{\partial^2}{\partial \zeta^2}(\Delta\phi) = \frac{2}{\zeta_{k+1} - \zeta_{k-1}} \left[ \frac{\Delta\phi_{k+1} - \Delta\phi_k}{\zeta_{k+1} - \zeta_k} - \frac{\Delta\phi_k - (\Delta\phi_{k-1} - \Gamma^{n+1} + \Gamma^*)}{\zeta_k - \zeta_{k-1}} \right] \quad (122a)$$

at grid points in the plane above the wake and by defining

$$\frac{\partial^2}{\partial \zeta^2}(\Delta\phi) = \frac{2}{\zeta_{k+1} - \zeta_{k-1}} \left[ \frac{(\Delta\phi_{k+1} - \Gamma^{n+1} + \Gamma^*) - \Delta\phi_k}{\zeta_{k+1} - \zeta_k} - \frac{\Delta\phi_k - \Delta\phi_{k-1}}{\zeta_k - \zeta_{k-1}} \right] \quad (122b)$$

at grid points in the plane below the wake. Since the circulation terms are known quantities, they are brought to the right-hand side of the  $\zeta$ -sweep equation. The tridiagonal coefficients of the  $\zeta$ -sweep are unchanged consequently, and the right-hand side becomes

$$\Delta\bar{\phi} - \frac{\Delta t_1 \Delta t_2}{2A} \frac{2}{\zeta_{k+1} - \zeta_{k-1}} \frac{1}{\zeta_k - \zeta_{k-1}} (\Gamma^{n+1} - \Gamma^*) \quad (123a)$$

at the grid points in the plane above the wake and

$$\Delta\bar{\phi} + \frac{\Delta t_1 \Delta t_2}{2A} \frac{2}{\zeta_{k+1} - \zeta_{k-1}} \frac{1}{\zeta_{k+1} - \zeta_k} (\Gamma^{n+1} - \Gamma^*) \quad (123b)$$

at grid points in the plane below the wake.

The convection of entropy is governed by the same type of equation as the convection of circulation. Namely, the entropy is determined by

$$s_{x_{i-1/2}}^{n+1} + s_{t_{i-1/2}}^{n+1} = 0 \quad (124)$$

Approximating the derivatives of equation (124) in the same way as the derivatives of circulation results in

$$\begin{aligned} s_i^{n+1} = & \left( \xi_{x_{i-1/2,j}} \frac{1}{\xi_i - \xi_{i-1}} + \frac{1}{2} \frac{2\Delta t_1 \Delta t_2}{\Delta t_1 + \Delta t_2} \frac{1}{\Delta t_1} \right)^{-1} \left[ \xi_{x_{i-1/2,j}} \frac{s_{i-1}^{n+1}}{\xi_i - \xi_{i-1}} \right. \\ & + \frac{1}{2} \left( -\frac{2}{\Delta t_1 + \Delta t_2} \frac{\Delta t_1 + \Delta t_2}{\Delta t_1} \frac{s_i^n}{\Delta t_1} - \frac{\Delta t_1}{\Delta t_1 + \Delta t_2} \frac{s_i^n - s_i^{n-1}}{\Delta t_2} \right. \\ & \left. \left. + \frac{2}{\Delta t_1 + \Delta t_2} \frac{\Delta t_1 + \Delta t_2}{\Delta t_1} \frac{s_{i-1}^{n+1} - s_{i-1}^n}{\Delta t_1} - \frac{\Delta t_1}{\Delta t_1 + \Delta t_2} \frac{s_{i-1}^n - s_{i-1}^{n-1}}{\Delta t_2} \right) \right] \quad (125) \end{aligned}$$

Through use of equation (125), the entropy is convected downstream by calculating  $s_i^{n+1}$  for all grid points downstream of shocks beginning with the value at the shock determined by the Rankine-Hugoniot shock jump relation (eq. (19)).

Modifications to the  $L_\zeta$  operator, similar to the modifications made to the  $L_\xi$  and  $L_\eta$  operators, are also required to accommodate the flow-tangency boundary conditions for bodies. For grid points that lie inside the computational box that is used to model a body,

$$\Delta\phi = 0 \quad (126)$$

since there is no flow. This results in the following tridiagonal coefficients and right-hand side:

$$c_k = 0 \quad (127a)$$

$$d_k = 1 \quad (127b)$$

$$e_k = 0 \quad (127c)$$

$$R_k = 0 \quad (127d)$$

For grid points in the plane  $k$  that is above the top surface of the computational box,

$$\frac{\partial}{\partial \zeta}(\Delta\phi)_{k-1/2} = 0 \quad (128)$$

which results in the following tridiagonal coefficients:

$$c_k = 0 \quad (129a)$$

$$d_k = 1 + \frac{\Delta t_1 \Delta t_2}{2A} \frac{2}{\zeta_{k+1} - \zeta_{k-1}} \frac{1}{\zeta_{k+1} - \zeta_k} \quad (129b)$$

$$e_k = -\frac{\Delta t_1 \Delta t_2}{2A} \frac{2}{\zeta_{k+1} - \zeta_{k-1}} \frac{1}{\zeta_{k+1} - \zeta_k} \quad (129c)$$

Similarly, for grid points in the plane  $k$  that is below the bottom surface of the computational box,

$$c_k = -\frac{\Delta t_1 \Delta t_2}{2A} \frac{2}{\zeta_{k+1} - \zeta_{k-1}} \frac{1}{\zeta_k - \zeta_{k-1}} \quad (130a)$$

$$d_k = 1 + \frac{\Delta t_1 \Delta t_2}{2A} \frac{2}{\zeta_{k+1} - \zeta_{k-1}} \frac{1}{\zeta_k - \zeta_{k-1}} \quad (130b)$$

$$e_k = 0 \quad (130c)$$

These modifications (eqs. (126) to (130)) are made for both the time-linearization and subiteration steps of the AF algorithm since the current implementation can only treat steady boundary conditions for bodies.

## Difference Equations for the Residual

The finite-difference equations for the residual are presented in this section. These equations are derived by first rewriting the residual in the following general form:

$$R = -\xi_x \frac{\Delta t_1 \Delta t_2}{2A} \left( \frac{\partial g_0}{\partial t} + \frac{\partial g_1}{\partial \xi} + \frac{\partial g_2}{\partial \eta} + \frac{\partial g_3}{\partial \zeta} \right) \quad (131)$$

where

$$g_0 = -\frac{A}{\xi_x} \phi_t^* - B \phi_\xi^* \quad (132a)$$

$$g_1 = E \phi_x^* + F (\phi_x^*)^2 + G (\phi_y^*)^2 + \frac{\xi_y}{\xi_x} (1 + H \phi_x^*) \phi_y^* \quad (132b)$$

$$g_2 = \frac{1}{\xi_x} (1 + H \phi_x^*) \phi_y^* \quad (132c)$$

$$g_3 = \frac{1}{\xi_x} \phi_z^* \quad (132d)$$

However, in the nonisentropic formulation,

$$g_1 = (\gamma + 1) M_\infty^2 Q \left( V V^s - \frac{1}{2} V^2 \right) + G \left( \phi_y^* \right)^2 + \frac{\xi_y}{\xi_x} (1 + H \phi_x^*) \phi_y^* \quad (132e)$$

Also, the spatial fluxes  $g_1$ ,  $g_2$ , and  $g_3$ , which are in the  $\xi$ -,  $\eta$ -, and  $\zeta$ -coordinate directions, respectively, have been written in terms of the  $x$ ,  $y$ , and  $z$  physical coordinates for convenience and computational efficiency (as is made evident in the following subsections).

### $\partial g_0 / \partial t$ Term

The  $\partial g_0 / \partial t$  term is treated by considering separately each of the two derivatives that make up this term in a manner that is consistent with the treatment of similar terms in the  $L_\xi$  operator. In other words, the time term is expressed as

$$\frac{\partial g_0}{\partial t} = -\frac{A}{\xi_{x_{i,j}}} \phi_{tt_i}^* - B \phi_{\xi t_i}^* \quad (133)$$

where the  $\phi_{tt_i}^*$  and  $\phi_{\xi t_i}^*$  derivatives are then approximated by finite-difference formulas that account for variable time stepping given by

$$\begin{aligned} \phi_{tt_i}^* = & \frac{\Delta t_1 + \Delta t_2}{\Delta t_2} \left[ \frac{2}{\Delta t_1 + \Delta t_2} \frac{\Delta t_2 \phi_i^* - (\Delta t_1 + \Delta t_2) \phi_i^n + \Delta t_1 \phi_i^{n-1}}{\Delta t_1 \Delta t_2} \right] \\ & - \frac{\Delta t_1}{\Delta t_2} \left[ \frac{2}{\Delta t_2 + \Delta t_3} \frac{\Delta t_3 \phi_i^n - (\Delta t_2 + \Delta t_3) \phi_i^{n-1} + \Delta t_2 \phi_i^{n-2}}{\Delta t_2 \Delta t_3} \right] \end{aligned} \quad (134)$$

$$\begin{aligned} \phi_{\xi t_i}^* = & \frac{2}{\xi_{i+1} - \xi_{i-1}} \left[ \frac{2 \Delta t_1 + \Delta t_2}{\Delta t_1 + \Delta t_2} \frac{(\phi_i^* - \phi_{i-1}^*) - (\phi_i^n - \phi_{i-1}^n)}{\Delta t_1} \right. \\ & \left. - \frac{\Delta t_1}{\Delta t_1 + \Delta t_2} \frac{(\phi_i^n - \phi_{i-1}^n) - (\phi_i^{n-1} - \phi_{i-1}^{n-1})}{\Delta t_2} \right] \end{aligned} \quad (135)$$

Note that the spatial derivative in  $\phi_{\xi t_i}^*$  is backward differenced consistent with the treatment of the similar term in the  $L_\xi$  operator. Furthermore, for time stepping involving a constant step size (i.e.,  $\Delta t = \Delta t_1 = \Delta t_2 = \Delta t_3$ ), equations (134) and (135) simplify to the more familiar formulas given by

$$\phi_{tt_i}^* = \frac{2\phi_i^* - 5\phi_i^n + 4\phi_i^{n-1} - \phi_i^{n-2}}{\Delta t^2} \quad (136)$$

$$\phi_{\xi t_i}^* = \frac{2}{\xi_{i+1} - \xi_{i-1}} \frac{3(\phi_i^* - \phi_{i-1}^*) - 4(\phi_i^n - \phi_{i-1}^n) + (\phi_i^{n-1} - \phi_{i-1}^{n-1})}{2 \Delta t} \quad (137)$$

### $\partial g_1 / \partial \xi$ Term

The  $\partial g_1 / \partial \xi$  term is treated by first considering the flux  $g_1$  as being the sum of two fluxes, so that

$$\frac{\partial g_1}{\partial \xi} = \frac{\partial g_1^{\text{EO}}}{\partial \xi} + \frac{\partial g_1^{\text{CD}}}{\partial \xi} \quad (138)$$

where

$$g_1^{\text{EO}} = E\phi_x^* + F(\phi_x^*)^2 \quad (139)$$

for the isentropic formulation,

$$g_1^{\text{EO}} = (\gamma + 1)M_\infty^2 Q \left( VV^s - \frac{1}{2}V^2 \right) \quad (140)$$

for the nonisentropic formulation, and

$$g_1^{\text{CD}} = G(\phi_y^*)^2 + \frac{\xi_y}{\xi_x} (1 + H\phi_x^*) \phi_y^* \quad (141)$$

In equation (139) or equation (140),  $g_1^{\text{EO}}$  is either centrally differenced at subsonic points or backward differenced at supersonic points according to the Engquist-Osher (EO) type-dependent mixed-difference operator, and  $g_1^{\text{CD}}$  is always centrally differenced (CD) independent of the local speed of the flow. Specifically, the derivative of the first part of the flux is represented by the following EO type-dependent formula:

$$\begin{aligned} \frac{\partial g_1^{\text{EO}}}{\partial \xi} = \frac{2}{\xi_{i+1} - \xi_{i-1}} & \left[ (1 - \varepsilon_{i+1/2}) g_{1_{i+1/2}}^{\text{EO}} + (2\varepsilon_{i-1/2} - 1) g_{1_{i-1/2}}^{\text{EO}} \right. \\ & \left. - \varepsilon_{i-3/2} g_{1_{i-3/2}}^{\text{EO}} + (\varepsilon_{i+1/2} - 2\varepsilon_{i-1/2} + \varepsilon_{i-3/2}) g_1^s \right] \end{aligned} \quad (142)$$

where, in the isentropic formulation,

$$g_{1_{i-1/2}}^{\text{EO}} = E\phi_{x_{i-1/2,j}}^* + F(\phi_{x_{i-1/2,j}}^*)^2 \quad (143)$$

$$\varepsilon_{i-1/2} = \begin{cases} 0 & (\phi_{x_{i-1/2,j}}^* \leq \phi_x^s) \\ 1 & (\phi_{x_{i-1/2,j}}^* > \phi_x^s) \end{cases}$$

and the sonic reference flux  $g_1^s$  is defined by

$$g_1^s = E\phi_x^s + F(\phi_x^s)^2 = \frac{-E^2}{4F} \quad (144)$$

In the nonisentropic formulation,

$$g_{1_{i-1/2}}^{\text{EO}} = (\gamma + 1)M_\infty^2 Q \left( V_{i-1/2,j} V^s - \frac{1}{2}V_{i-1/2,j}^2 \right) \quad (145)$$

$$\varepsilon_{i-1/2,j} = \begin{cases} 0 & (V_{i-1/2,j} \leq V^s) \\ 1 & (V_{i-1/2,j} > V^s) \end{cases}$$

$$V_{i-1/2,j} = \frac{\phi_{x_{i-1/2,j}}^*}{1 + K_v \phi_{x_{i-1/2,j}}^*}$$

and the sonic reference flux is defined by

$$g_1^s = \frac{\gamma + 1}{2} M_\infty^2 Q V^s \quad (146)$$

The derivative of the second part of the flux is represented by a central-difference formula involving the flux  $g_1^{\text{CD}}$  evaluated at the half-node points in the  $\xi$ -direction according to

$$\frac{\partial g_1^{\text{CD}}}{\partial \xi} = \frac{2}{\xi_{i+1} - \xi_{i-1}} (g_{1,i+1/2,j}^{\text{CD}} - g_{1,i-1/2,j}^{\text{CD}}) \quad (147)$$

where

$$g_{1,i-1/2,j}^{\text{CD}} = G \left( \phi_{y_{i-1/2,j}}^* \right)^2 + \frac{\xi_{y_{i-1/2,j}}}{\xi_{x_{i-1/2,j}}} \left( 1 + H \phi_{x_{i-1/2,j}}^* \right) \phi_{y_{i-1/2,j}}^* \quad (148)$$

The  $\partial g_1^{\text{CD}}/\partial \xi$  term, however, is defined differently to impose the symmetry condition (normally taken to be  $j = 1$ ). This results from requiring that

$$\phi_{y_{i-1/2,j}}^* = 0 \quad (149)$$

which implies that

$$\frac{\partial g_1^{\text{CD}}}{\partial \xi} = 0 \quad (150)$$

for grid points in the symmetry plane.

#### $\partial g_2/\partial \eta$ Term

The  $\partial g_2/\partial \eta$  term is represented by a central-difference formula involving the flux  $g_2$  evaluated at the half-node points in the  $\eta$ -direction according to

$$\frac{\partial g_2}{\partial \eta} = \frac{2}{\eta_{j+1} - \eta_{j-1}} (g_{2,i,j+1/2} - g_{2,i,j-1/2}) \quad (151)$$

where

$$g_{2,i,j-1/2} = \frac{1}{\xi_{x_{i,j-1/2}}} \left( 1 + H \phi_{x_{i,j-1/2}}^* \right) \phi_{y_{i,j-1/2}}^* \quad (152)$$

The  $\partial g_2/\partial \eta$  term, however, is defined differently to impose the symmetry condition ( $j = J$ ; normally taken to be  $J = 1$ ). Here,

$$\phi_{y_{i,J-1/2}}^* = -\phi_{y_{i,J+1/2}}^* \quad (153)$$

and

$$\phi_{x_{i,J-1/2}}^* = \phi_{x_{i,J+1/2}}^* \quad (154)$$

These two conditions imply that

$$g_{2,i,J-1/2} = -g_{2,i,J+1/2} \quad (155)$$

so that finally at the symmetry plane

$$\frac{\partial g_2}{\partial \eta} = \frac{2}{\eta_{J+1} - \eta_J} g_{2,i,J+1/2} \quad (156)$$

#### $\partial g_3/\partial \zeta$ Term

The  $\partial g_3/\partial \zeta$  term is represented by a central-difference formula involving the flux  $g_3$  evaluated at the half-node points in the  $\zeta$ -direction according to

$$\frac{\partial g_3}{\partial \zeta} = \frac{2}{\zeta_{k+1} - \zeta_{k-1}} (g_{3,i,j,k+1/2} - g_{3,i,j,k-1/2}) \quad (157)$$



where

$$g_{3,i,j,k-1/2} = \frac{1}{\xi_{x_{i,j}}} \phi_{z_{k-1/2}}^* \quad (158)$$

The  $\partial g_3 / \partial \zeta$  term, however, is defined differently when the lifting-surface flow-tangency and wake boundary conditions and the flow-tangency conditions for bodies are imposed. This term is defined differently for grid points in the planes directly above and below the lifting surface and its wake and directly above and below the computational surfaces used to model bodies, since the  $z$ -component of the disturbance velocity ( $\phi_z^*$ ) is modified there, as discussed in detail previously.

## Difference Equations for the Far-Field Boundary Conditions

The finite-difference equations for the far-field boundary conditions are presented in this section. These conditions involve the upstream, downstream, far-spanwise, upper, and lower boundaries of the grid. All these boundaries except for the upstream boundary are represented by nonreflecting conditions. At the upstream boundary the flow is assumed to be free stream, and consequently an undisturbed flow condition is prescribed.

### Upstream Boundary

The upstream boundary condition is implemented during the  $\xi$ -sweep of the AF solution procedure to determine values of the intermediate potential  $\bar{\phi}$  on the extreme upstream plane of grid points ( $i = 1$ ). The boundary condition (eq. (13a)) is applied along the extreme grid plane, which leads to the trivial equation

$$\Delta \bar{\phi} = 0 \quad (159)$$

The equation may be written for solution in quadradiagonal form (eq. (89)) as

$$b_i \Delta \bar{\phi}_{i-2} + c_i \Delta \bar{\phi}_{i-1} + d_i \Delta \bar{\phi}_i + e_i \Delta \bar{\phi}_{i+1} = -R_i$$

where

$$b_i = 0 \quad (160a)$$

$$c_i = 0 \quad (160b)$$

$$d_i = 1 \quad (160c)$$

$$e_i = 0 \quad (160d)$$

$$R_i = 0 \quad (160e)$$

### Downstream Boundary

The downstream boundary condition is implemented during the  $\xi$ -sweep of the AF solution procedure to determine values of the intermediate potential  $\bar{\phi}$  on the extreme downstream plane of grid points ( $i = \text{NXT}$ ). The condition (eq. (13b)) is applied midway between the extreme and adjacent grid planes according to

$$P_{i-1/2} (\bar{\phi}_i)_{i-1/2} + \xi_{x_{i-1/2}} (\bar{\phi}_\xi)_{i-1/2} = 0 \quad (161)$$

where

$$P_{i-1/2} = \frac{1}{2} \left( \frac{-B}{C_{i-1/2}} + \frac{D_{i-1/2}}{\sqrt{C_{i-1/2}}} \right) \quad (162a)$$

$$D_{i-1/2} = \left( 4A + \frac{B^2}{C_{i-1/2}} \right)^{1/2} \quad (162b)$$

$$C_{i-1/2} = E + 2F\phi_{x_{i-1/2},j}^* \quad (162c)$$

With second-order-accurate central-difference and one-sided-difference approximations used for the space and time derivatives, respectively, the difference equation for equation (161) becomes

$$\begin{aligned} \frac{1}{2}P_{i-1/2} & \left\{ \left[ \frac{2\Delta t_1 + \Delta t_2}{\Delta t_1 + \Delta t_2} \left( \frac{\bar{\phi}_i - \phi_i^n}{\Delta t_1} \right) - \frac{\Delta t_1}{\Delta t_1 + \Delta t_2} \left( \frac{\phi_i^n - \phi_i^{n-1}}{\Delta t_2} \right) \right] \right. \\ & + \left. \left[ \frac{2\Delta t_1 + \Delta t_2}{\Delta t_1 + \Delta t_2} \left( \frac{\bar{\phi}_{i-1} - \phi_{i-1}^n}{\Delta t_1} \right) - \frac{\Delta t_1}{\Delta t_1 + \Delta t_2} \left( \frac{\phi_{i-1}^n - \phi_{i-1}^{n-1}}{\Delta t_2} \right) \right] \right\} \\ & + \xi_{x_{i-1/2}} \left( \frac{\bar{\phi}_i - \bar{\phi}_{i-1}}{\xi_i - \xi_{i-1}} \right) = 0 \end{aligned} \quad (163)$$

By linearizing consistently with the  $\xi$ -sweep of the AF procedure, the difference equation may be rewritten for solution in quadradiagonal form (eq. (89)) as

$$b_i \Delta \bar{\phi}_{i-2} + c_i \Delta \bar{\phi}_{i-1} + d_i \Delta \bar{\phi}_i + e_i \Delta \bar{\phi}_{i+1} = -R_i$$

where

$$b_i = 0 \quad (164a)$$

$$c_i = \frac{2\Delta t_1 + \Delta t_2}{2\Delta t_1(\Delta t_1 + \Delta t_2)} P_{i-1/2} - \xi_{x_{i-1/2},j} \frac{1}{\xi_i - \xi_{i-1}} \quad (164b)$$

$$d_i = \frac{2\Delta t_1 + \Delta t_2}{2\Delta t_1(\Delta t_1 + \Delta t_2)} P_{i-1/2} + \xi_{x_{i-1/2},j} \frac{1}{\xi_i - \xi_{i-1}} \quad (164c)$$

$$e_i = 0 \quad (164d)$$

and

$$\begin{aligned} R_i &= \frac{P_{i-1/2}}{2(\Delta t_1 + \Delta t_2)} \left[ \frac{2\Delta t_1 + \Delta t_2}{\Delta t_1} (\phi_i^* - \phi_i^n + \phi_{i-1}^* - \phi_{i-1}^n) \right. \\ & \quad \left. - \frac{\Delta t_1}{\Delta t_2} (\phi_i^n - \phi_i^{n-1} + \phi_{i-1}^n - \phi_{i-1}^{n-1}) \right] + \phi_{x_{i-1/2}}^* \end{aligned} \quad (164e)$$

After the  $\zeta$ -sweep of the AF solution procedure is completed, the potentials on the downstream boundary must be recomputed (since the potentials on the adjacent plane of grid points have changed values because of the  $\eta$ - and  $\zeta$ -sweeps) according to

$$\Delta \phi_i = \frac{-1}{d_i} (R_i + c_i \Delta \phi_{i-1}) \quad (165)$$

### Far-Spanwise Boundary

The far-spanwise boundary condition is implemented during the  $\eta$ -sweep of the AF solution procedure to determine values of the intermediate potential  $\bar{\phi}$  on the extreme spanwise plane of grid

points ( $j = \text{NYT}$ ). The condition (eq. (13e)) is applied midway between the extreme and adjacent grid planes according to

$$\frac{1}{2}D_{j-1/2}(\bar{\bar{\phi}}_t)_{j-1/2} + \xi_{y_{j-1/2}}(\bar{\bar{\phi}}_\xi)_{j-1/2} + (\bar{\bar{\phi}}_\eta)_{j-1/2} = 0 \quad (166)$$

where

$$D_{j-1/2} = \left(4A + \frac{B^2}{C_{j-1/2}}\right)^{1/2} \quad (167a)$$

$$C_{j-1/2} = E + 2F\phi_{x_{i,j-1/2}}^* \quad (167b)$$

With second-order-accurate central-difference and one-sided-difference approximations used for the space and time derivatives, respectively, the difference equation for equation (166) becomes

$$\begin{aligned} \frac{1}{4}D_{j-1/2} \left\{ \left[ \frac{2\Delta t_1 + \Delta t_2}{\Delta t_1 + \Delta t_2} \left( \frac{\bar{\bar{\phi}}_j - \phi_j^n}{\Delta t_1} \right) - \frac{\Delta t_1}{\Delta t_1 + \Delta t_2} \left( \frac{\phi_j^n - \phi_j^{n-1}}{\Delta t_2} \right) \right] \right. \\ \left. + \left[ \frac{2\Delta t_1 + \Delta t_2}{\Delta t_1 + \Delta t_2} \left( \frac{\bar{\bar{\phi}}_{j-1} - \phi_{j-1}^n}{\Delta t_1} \right) - \frac{\Delta t_1}{\Delta t_1 + \Delta t_2} \left( \frac{\phi_{j-1}^n - \phi_{j-1}^{n-1}}{\Delta t_2} \right) \right] \right\} \\ + \xi_{y_{i,j-1/2}} \frac{\phi_{i+1,j}^* - \phi_{i-1,j}^* + \phi_{i+1,j-1}^* - \phi_{i-1,j-1}^*}{2(\xi_{i+1} - \xi_{i-1})} + \frac{\bar{\bar{\phi}}_j - \bar{\bar{\phi}}_{j-1}}{\eta_j - \eta_{j-1}} = 0 \end{aligned} \quad (168)$$

By linearizing consistently with the  $\eta$ -sweep of the AF procedure, the difference equation may be rewritten for solution in tridiagonal form as

$$c_j \Delta \bar{\bar{\phi}}_{j-1} + d_j \Delta \bar{\bar{\phi}}_j + e_j \Delta \bar{\bar{\phi}}_{j+1} = -R_j \quad (169)$$

where

$$c_j = \frac{2\Delta t_1 + \Delta t_2}{4\Delta t_1(\Delta t_1 + \Delta t_2)} D_{j-1/2} - \frac{1}{\eta_j - \eta_{j-1}} \quad (170a)$$

$$d_j = \frac{2\Delta t_1 + \Delta t_2}{4\Delta t_1(\Delta t_1 + \Delta t_2)} D_{j-1/2} + \frac{1}{\eta_j - \eta_{j-1}} \quad (170b)$$

$$e_j = 0 \quad (170c)$$

and

$$\begin{aligned} R_j = \frac{D_{j-1/2}}{4(\Delta t_1 + \Delta t_2)} \left[ \frac{2\Delta t_1 + \Delta t_2}{\Delta t_1} (\phi_j^* - \phi_j^n + \phi_{j-1}^* - \phi_{j-1}^n) \right. \\ \left. - \frac{\Delta t_1}{\Delta t_2} (\phi_j^n - \phi_j^{n-1} + \phi_{j-1}^n - \phi_{j-1}^{n-1}) \right] + \phi_{y_{i,j-1/2}}^* \end{aligned} \quad (170d)$$

After the  $\zeta$ -sweep of the AF solution procedure is completed, the potentials on the far-spanwise boundary ( $j = \text{NYT}$ ) must be recomputed (since the potentials on the adjacent plane of grid points have changed values because of the  $\zeta$ -sweep) according to

$$\Delta \phi_j = \frac{-1}{d_j} (R_j + c_j \Delta \phi_{j-1}) \quad (171)$$

For full-span modeling, a similar boundary condition is imposed to determine values of the intermediate potential  $\bar{\bar{\phi}}$  on the  $j = 1$  plane of grid points. The condition (eq. (13f)) is applied between the extreme ( $j = 1$ ) and adjacent grid planes according to

$$\frac{1}{2}D_{j+1/2}(\bar{\bar{\phi}}_t)_{j+1/2} - \xi_{y_{j+1/2}}(\bar{\bar{\phi}}_\xi)_{j+1/2} - (\bar{\bar{\phi}}_\eta)_{j+1/2} = 0 \quad (172)$$

where

$$D_{j+1/2} = \left(4A + \frac{B^2}{C_{j+1/2}}\right)^{1/2} \quad (173a)$$

$$C_{j+1/2} = E + 2F\phi_{x_{i,j+1/2}}^* \quad (173b)$$

With second-order-accurate central-difference and one-sided-difference approximations used for the space and time derivatives, respectively, the difference equation for equation (172) becomes

$$\begin{aligned} \frac{1}{4}D_{j+1/2} & \left\{ \left[ \frac{2\Delta t_1 + \Delta t_2}{\Delta t_1 + \Delta t_2} \left( \frac{\bar{\bar{\phi}}_j - \phi_j^n}{\Delta t_1} \right) - \frac{\Delta t_1}{\Delta t_1 + \Delta t_2} \left( \frac{\phi_j^n - \phi_j^{n-1}}{\Delta t_2} \right) \right] \right. \\ & + \left. \left[ \frac{2\Delta t_1 + \Delta t_2}{\Delta t_1 + \Delta t_2} \left( \frac{\bar{\bar{\phi}}_{j+1} - \phi_{j+1}^n}{\Delta t_1} \right) - \frac{\Delta t_1}{\Delta t_1 + \Delta t_2} \left( \frac{\phi_{j+1}^n - \phi_{j+1}^{n-1}}{\Delta t_2} \right) \right] \right\} \\ & - \xi_{y_{i,j+1/2}} \frac{\phi_{i+1,j+1}^* - \phi_{i-1,j+1}^* + \phi_{i+1,j}^* - \phi_{i-1,j}^*}{2(\xi_{i+1} - \xi_{i-1})} - \frac{\bar{\bar{\phi}}_{j+1} - \bar{\bar{\phi}}_j}{\eta_{j+1} - \eta_j} = 0 \end{aligned} \quad (174)$$

By linearizing consistently with the  $\eta$ -sweep of the AF procedure, the difference equation may be rewritten for solution in tridiagonal form (eq. (169)) as

$$c_j \Delta \bar{\bar{\phi}}_{j-1} + d_j \Delta \bar{\bar{\phi}}_j + e_j \Delta \bar{\bar{\phi}}_{j+1} = -R_j$$

where

$$c_j = 0 \quad (175a)$$

$$d_j = \frac{2\Delta t_1 + \Delta t_2}{4\Delta t_1(\Delta t_1 + \Delta t_2)} D_{j+1/2} - \frac{1}{\eta_{j+1} - \eta_j} \quad (175b)$$

$$e_j = \frac{2\Delta t_1 + \Delta t_2}{4\Delta t_1(\Delta t_1 + \Delta t_2)} D_{j+1/2} + \frac{1}{\eta_{j+1} - \eta_j} \quad (175c)$$

and

$$\begin{aligned} R_j = \frac{D_{j+1/2}}{4(\Delta t_1 + \Delta t_2)} & \left[ \frac{2\Delta t_1 + \Delta t_2}{\Delta t_1} (\phi_j^* - \phi_j^n + \phi_{j+1}^* - \phi_{j+1}^n) \right. \\ & \left. - \frac{\Delta t_1}{\Delta t_2} (\phi_j^n - \phi_j^{n-1} + \phi_{j+1}^n - \phi_{j+1}^{n-1}) \right] - \phi_{y_{i,j+1/2}}^* \end{aligned} \quad (175d)$$

After the  $\zeta$ -sweep of the AF solution procedure is completed, the potentials on the far-spanwise boundary ( $j = 1$ ) must be recomputed (since the potentials on the adjacent plane of grid points

have changed values because of the  $\zeta$ -sweep) according to

$$\Delta\phi_j = \frac{-1}{d_j} (R_j + e_j \Delta\phi_{j+1}) \quad (176)$$

### Upper Boundary

The upper boundary condition is implemented during the  $\zeta$ -sweep of the AF solution procedure to determine values of the potential  $\phi^{n+1}$  on the extreme upper plane of grid points ( $k = \text{NZT}$ ). The condition (eq. (13c)) is applied midway between the extreme and adjacent grid planes according to

$$\frac{1}{2} D_{k-1/2} (\phi_t^{n+1})_{k-1/2} + (\phi_\zeta^{n+1})_{k-1/2} = 0 \quad (177)$$

where

$$D_{k-1/2} = \left( 4A + \frac{B^2}{C_{k-1/2}} \right)^{1/2} \quad (178a)$$

$$C_{k-1/2} = E + F (\phi_{x_{i,k}}^* + \phi_{x_{i,k-1}}^*) \quad (178b)$$

$$\phi_{x_{i,k}}^* = \xi_{x_{i,j}} \frac{\phi_{i+1,k}^* - \phi_{i-1,k}^*}{\xi_{i+1} - \xi_{i-1}} \quad (178c)$$

With second-order-accurate central-difference and one-sided-difference approximations used for the space and time derivatives, respectively, the difference equation for equation (177) becomes

$$\begin{aligned} \frac{1}{4} D_{k-1/2} & \left\{ \left[ \frac{2 \Delta t_1 + \Delta t_2}{\Delta t_1 + \Delta t_2} \left( \frac{\phi_k^{n+1} - \phi_k^n}{\Delta t_1} \right) - \frac{\Delta t_1}{\Delta t_1 + \Delta t_2} \left( \frac{\phi_k^n - \phi_k^{n-1}}{\Delta t_2} \right) \right] \right. \\ & + \left[ \frac{2 \Delta t_1 + \Delta t_2}{\Delta t_1 + \Delta t_2} \left( \frac{\phi_{k-1}^{n+1} - \phi_{k-1}^n}{\Delta t_1} \right) - \frac{\Delta t_1}{\Delta t_1 + \Delta t_2} \left( \frac{\phi_{k-1}^n - \phi_{k-1}^{n-1}}{\Delta t_2} \right) \right] \Big\} \\ & + \frac{\phi_k^{n+1} - \phi_{k-1}^{n+1}}{\zeta_k - \zeta_{k-1}} = 0 \end{aligned} \quad (179)$$

By linearizing consistently with the  $\zeta$ -sweep of the AF procedure, the difference equation may be rewritten for solution in tridiagonal form as

$$c_k \Delta\phi_{k-1} + d_k \Delta\phi_k + e_k \Delta\phi_{k+1} = -R_k \quad (180)$$

where

$$c_k = \frac{2 \Delta t_1 + \Delta t_2}{4 \Delta t_1 (\Delta t_1 + \Delta t_2)} D_{k-1/2} - \frac{1}{\zeta_k - \zeta_{k-1}} \quad (181a)$$

$$d_k = \frac{2 \Delta t_1 + \Delta t_2}{4 \Delta t_1 (\Delta t_1 + \Delta t_2)} D_{k-1/2} + \frac{1}{\zeta_k - \zeta_{k-1}} \quad (181b)$$

$$e_k = 0 \quad (181c)$$

and

$$R_k = \frac{D_{k-1/2}}{4(\Delta t_1 + \Delta t_2)} \left[ \frac{2\Delta t_1 + \Delta t_2}{\Delta t_1} (\phi_k^* - \phi_k^n + \phi_{k-1}^* - \phi_{k-1}^n) - \frac{\Delta t_1}{\Delta t_2} (\phi_k^n - \phi_k^{n-1} + \phi_{k-1}^n - \phi_{k-1}^{n-1}) \right] + \phi_{z_{k-1/2}}^* \quad (181d)$$

### Lower Boundary

The lower boundary condition is implemented during the  $\zeta$ -sweep of the AF solution procedure to determine values of the potential  $\phi^{n+1}$  on the extreme lower plane of grid points ( $k = 1$ ). The condition (eq. (13d)) is applied midway between the extreme and adjacent grid planes according to

$$\frac{1}{2}D_{k+1/2}(\phi_t^{n+1})_{k+1/2} - (\phi_\zeta^{n+1})_{k+1/2} = 0 \quad (182)$$

where

$$D_{k+1/2} = \left( 4A + \frac{B^2}{C_{k+1/2}} \right)^{1/2} \quad (183a)$$

$$C_{k+1/2} = E + F(\phi_{x_{i,k}}^* + \phi_{x_{i,k+1}}^*) \quad (183b)$$

$$\phi_{x_{i,k}}^* = \xi_{x_{i,j}} \frac{\phi_{i+1,k}^* - \phi_{i-1,k}^*}{\xi_{i+1} - \xi_{i-1}} \quad (183c)$$

With second-order-accurate central-difference and one-sided-difference approximations used for the space and time derivatives, respectively, the difference equation for equation (182) becomes

$$\begin{aligned} \frac{1}{4}D_{k+1/2} \left\{ \left[ \frac{2\Delta t_1 + \Delta t_2}{\Delta t_1 + \Delta t_2} \left( \frac{\phi_{k+1}^{n+1} - \phi_{k+1}^n}{\Delta t_1} \right) - \frac{\Delta t_1}{\Delta t_1 + \Delta t_2} \left( \frac{\phi_{k+1}^n - \phi_{k+1}^{n-1}}{\Delta t_2} \right) \right] \right. \\ \left. + \left[ \frac{2\Delta t_1 + \Delta t_2}{\Delta t_1 + \Delta t_2} \left( \frac{\phi_k^{n+1} - \phi_k^n}{\Delta t_1} \right) - \frac{\Delta t_1}{\Delta t_1 + \Delta t_2} \left( \frac{\phi_k^n - \phi_k^{n-1}}{\Delta t_2} \right) \right] \right\} \\ - \frac{\phi_{k+1}^{n+1} - \phi_k^{n+1}}{\zeta_{k+1} - \zeta_k} = 0 \end{aligned} \quad (184)$$

By linearizing consistently with the  $\zeta$ -sweep of the AF procedure, the difference equation may be rewritten for solution in tridiagonal form (eq. (180)) as

$$c_k \Delta \phi_{k-1} + d_k \Delta \phi_k + e_k \Delta \phi_{k+1} = -R_k$$

where

$$c_k = 0 \quad (185a)$$

$$d_k = \frac{2\Delta t_1 + \Delta t_2}{4\Delta t_1(\Delta t_1 + \Delta t_2)} D_{k+1/2} + \frac{1}{\zeta_{k+1} - \zeta_k} \quad (185b)$$

$$e_k = \frac{2\Delta t_1 + \Delta t_2}{4\Delta t_1(\Delta t_1 + \Delta t_2)} D_{k+1/2} - \frac{1}{\zeta_{k+1} - \zeta_k} \quad (185c)$$

and

$$R_k = \frac{D_{k+1/2}}{4(\Delta t_1 + \Delta t_2)} \left[ \frac{2\Delta t_1 + \Delta t_2}{\Delta t_1} (\phi_{k+1}^* - \phi_{k+1}^n + \phi_k^* - \phi_k^n) - \frac{\Delta t_1}{\Delta t_2} (\phi_{k+1}^n - \phi_{k+1}^{n-1} + \phi_k^n - \phi_k^{n-1}) \right] - \phi_{z_{k+1/2}}^* \quad (185d)$$

## Concluding Remarks

A time-accurate approximate-factorization (AF) algorithm has been described for solution of the three-dimensional unsteady transonic small-disturbance equation. The AF algorithm consists of a time-linearization procedure coupled with a subiteration technique. The algorithm is the basis for the CAP-TSD (Computational Aeroelasticity Program-Transonic Small Disturbance) computer code, which was developed for unsteady aerodynamic and aeroelastic analyses of realistic aircraft configurations. The paper described details on the governing flow equations and boundary conditions, with an emphasis on documenting the finite-difference formulas of the AF algorithm.

NASA Langley Research Center  
Hampton, VA 23665-5225  
November 7, 1991

## References

1. Edwards, John W.; and Thomas, James L.: Computational Methods for Unsteady Transonic Flows. *Unsteady Transonic Aerodynamics*, David Nixon, ed., Volume 120 of *Progress in Astronautics and Aeronautics*, American Inst. of Aeronautics and Astronautics, Inc., c.1989, pp. 211-261.
2. Batina, John T.; Seidel, David A.; Bland, Samuel R.; and Bennett, Robert M.: Unsteady Transonic Flow Calculations for Realistic Aircraft Configurations. *J. Aircr.*, vol. 26, no. 1, Jan. 1989, pp. 21-28.
3. Batina, John T.: Efficient Algorithm for Solution of the Unsteady Transonic Small-Disturbance Equation. *J. Aircr.*, vol. 25, no. 7, July 1988, pp. 598-605.
4. Batina, John T.: Unsteady Transonic Algorithm Improvements for Realistic Aircraft Applications. *J. Aircr.*, vol. 26, no. 2, Feb. 1989, pp. 131-139.
5. Shankar, Vijaya; Ide, Hiroshi; Gorski, Joseph; and Osher, Stanley: A Fast, Time-Accurate, Unsteady Full Potential Scheme. *AIAA J.*, vol. 25, no. 2, Feb. 1987, pp. 230-238.
6. Batina, John T.: Unsteady Transonic Flow Calculations for Interfering Lifting Surface Configurations. *J. Aircr.*, vol. 23, no. 5, May 1986, pp. 422-430.
7. Boppe, C. W.; and Stern, M. A.: Simulated Transonic Flows for Aircraft With Nacelles, Pylons, and Winglets. AIAA-80-0130, Jan. 1980.
8. Batina, John T.: Unsteady Transonic Flow Calculations for Wing/Fuselage Configurations. *J. Aircr.*, vol. 23, no. 12, Dec. 1986, pp. 897-903.
9. Whitlow, Woodrow, Jr.: *Characteristic Boundary Conditions for Three-Dimensional Transonic Unsteady Aerodynamics*. NASA TM-86292, 1984.
10. Batina, John T.: Unsteady Transonic Small-Disturbance Theory Including Entropy and Vorticity Effects. *J. Aircr.*, vol. 26, no. 6, June 1989, pp. 531-538.
11. Fuglsang, Dennis F.; and Williams, Marc H.: Non-Isentropic Unsteady Transonic Small Disturbance Theory. *A Collection of Technical Papers, Part 2: Structural Dynamics—AIAA/ASME/ASCE/AHS 26th Structures, Structural Dynamics and Materials Conference*, 1985, pp. 83-95. (Available as AIAA-85-0600.)
12. Dang, Thong Q.; and Chen, Lee-Tzong: An Euler Correction Method for Two- and Three-Dimensional Transonic Flows. AIAA-87-0522, Jan. 1987.
13. Engquist, Bjorn; and Osher, Stanley: Stable and Entropy Satisfying Approximations for Transonic Flow Calculations. *Math. Comput.*, vol. 34, no. 149, Jan. 1980, pp. 45-75.







REPORT DOCUMENTATION PAGE			Form Approved OMB No. 0704-0188	
Public reporting burden for this collection of information is estimated to average 1 hour per response, including the time for reviewing instructions, searching existing data sources, gathering and maintaining the data needed, and completing and reviewing the collection of information. Send comments regarding this burden estimate or any other aspect of this collection of information, including suggestions for reducing this burden, to Washington Headquarters Services, Directorate for Information Operations and Reports, 1215 Jefferson Davis Highway, Suite 1204, Arlington, VA 22202-4302, and to the Office of Management and Budget, Paperwork Reduction Project (0704-0188), Washington, DC 20503.				
1. AGENCY USE ONLY(Leave blank)	2. REPORT DATE January 1992	3. REPORT TYPE AND DATES COVERED Technical Paper		
4. TITLE AND SUBTITLE A Finite-Difference Approximate-Factorization Algorithm for Solution of the Unsteady Transonic Small-Disturbance Equation		5. FUNDING NUMBERS WU 505-63-50-12		
6. AUTHOR(S) John T. Batina				
7. PERFORMING ORGANIZATION NAME(S) AND ADDRESS(ES) NASA Langley Research Center Hampton, VA 23665-5225		8. PERFORMING ORGANIZATION REPORT NUMBER L-16781		
9. SPONSORING/MONITORING AGENCY NAME(S) AND ADDRESS(ES) National Aeronautics and Space Administration Washington, DC 20546-0001		10. SPONSORING/MONITORING AGENCY REPORT NUMBER NASA TP-3129		
11. SUPPLEMENTARY NOTES				
12a. DISTRIBUTION/AVAILABILITY STATEMENT  <del>RESTRICTED</del>  Subject Category 02		12b. DISTRIBUTION CODE		
13. ABSTRACT (Maximum 200 words) A time-accurate approximate-factorization (AF) algorithm is described for solution of the three-dimensional unsteady transonic small-disturbance equation. The AF algorithm consists of a time-linearization procedure coupled with a subiteration technique. The algorithm is the basis for the CAP-TSD (Computational Aeroelasticity Program-Transonic Small Disturbance) computer code, which was developed for the analysis of unsteady aerodynamics and aeroelasticity of realistic aircraft configurations. The paper describes details on the governing flow equations and boundary conditions, with an emphasis on documenting the finite-difference formulas of the AF algorithm.				
14. SUBJECT TERMS Computational fluid dynamics; Unsteady aerodynamics; Transonic flow			15. NUMBER OF PAGES 36	
			16. PRICE CODE	
17. SECURITY CLASSIFICATION OF REPORT Unclassified	18. SECURITY CLASSIFICATION OF THIS PAGE Unclassified	19. SECURITY CLASSIFICATION OF ABSTRACT	20. LIMITATION OF ABSTRACT	



